Advances in Applied Mathematics and Mechanics
Adv. Appl. Math. Mech., Vol. **3**, No. 1, pp. 1-51

DOI: 10.4208/aamm.10-m1030
February 2011

REVIEW ARTICLE

A Brief Review of Elasticity and Viscoelasticity for Solids

Harvey Thomas Banks [1,*], Shuhua Hu [1] and Zackary R. Kenz [1]

[1] *Center for Research in Scientific Computation and Department of Mathematics, North Carolina State University, Raleigh, NC 27695-8212, USA*

Received 25 May 2010; Accepted (in revised version) 31 August 2010
Available online 15 October 2010

Abstract. There are a number of interesting applications where modeling elastic and/or viscoelastic materials is fundamental, including uses in civil engineering, the food industry, land mine detection and ultrasonic imaging. Here we provide an overview of the subject for both elastic and viscoelastic materials in order to understand the behavior of these materials. We begin with a brief introduction of some basic terminology and relationships in continuum mechanics, and a review of equations of motion in a continuum in both Lagrangian and Eulerian forms. To complete the set of equations, we then proceed to present and discuss a number of specific forms for the constitutive relationships between stress and strain proposed in the literature for both elastic and viscoelastic materials. In addition, we discuss some applications for these constitutive equations. Finally, we give a computational example describing the motion of soil experiencing dynamic loading by incorporating a specific form of constitutive equation into the equation of motion.

AMS subject classifications: 93A30, 74B05, 74B20, 74D05, 74D10

Key words: Mathematical modeling, Eulerian and Lagrangian formulations in continuum mechanics, elasticity, viscoelasticity, computational simulations in soil, constitutive relationships.

1 Introduction

Knowledge of the field of continuum mechanics is crucial when attempting to understand and describe the behavior of materials that completely fill the occupied space and thus act like a continuous medium. There are a number of interesting applications where modeling of elastic and viscoelastic materials is fundamental. One interest in particular is in describing the response of soil which experiences some sort of impact.

*Corresponding author.
URL: `http://www.ncsu.edu/crsc/htbanks/`
Email: htbanks@ncsu.edu (H. T. Banks), shu3@ncsu.edu (S. H. Hu), zrkenz@ncsu.edu (Z. R. Kenz)

This may result from buildings falling or being imploded, or even an intentionally introduced impact as part of land mine detection efforts (see [54, 56]). The chief interest is in determining what would happen to buried objects given a particular surface impact. In the case of a building implosion, there are concerns for buried infrastructure such as tunnels, pipes, or nearby building infrastructure. Investigations can be carried out to determine the likely forces on these buried objects to ensure that the force delivered into the soil will not damage other infrastructure. When detecting land mines, the methodology developed in the papers cited uses an impact on the ground to create Rayleigh surface waves that are subsequently changed upon interacting with a buried mine; this change in wave form might be detected through electromagnetic or acoustic means. Creating a model that accurately describes these Rayleigh waves is key to modeling and understanding the buried land mine situation. In both of these examples, one must study the soil properties, determine a valid constitutive relationship for the soil, and verify the accuracy of the model. One can then use the models to predict the results from different forces, soil properties, etc. Another application is the non-invasive detection of arterial stenosis (e.g., see [1, 3, 11, 38, 50]). In this study, blockages in the artery create turbulence in the blood flow, which then generates an acoustic wave with a normal and shear component. The acoustic wave propagates through the chest cavity until it reaches the chest wall, where a series of sensors detect the acceleration of the components of the wave. The data from the sensors can then be used to quickly determine the existence and perhaps the location of the blockages in the artery. This technique is inexpensive and non-invasive. For such a technology to be feasible, a mathematical model that describes the propagation of the acoustic wave from the stenosis to the chest wall will be necessary to correctly detect the location of a blockage.

The goal of this paper is to provide a brief introduction of both elastic and viscoelastic materials for those researchers with little or no previous knowledge on continuum mechanics but who are interested in studying the mechanics of materials. The materials that we are considering are simple (for example the stress at a given material point depends only on the history of the first order spatial gradient of the deformation in a small neighborhood of the material point and not on higher order spatial gradients) and non-aging (the microscopic changes during an experiment can be neglected in the basic model). Our presentation is part tutorial, part review but not a comprehensive survey of a truly enormous research literature. We rely on parts of the standard literature and discuss our view of generally accepted concepts. We present a discussion of topics we have found useful over the past several decades; hence approximately 20% of references are work from our group. We have not meant to ignore major applications in the many fine contributions of others; rather our presentation reflects a certain level of comfort in writing about efforts on which we have detailed knowledge and experience.

The introductory review is outlined as follows: in Section 2 some basic terminology (such as stress and strain) and relationships (e.g., the relationship between strain and displacement) of continuum mechanics are briefly described. In addition, we give

a brief overview of equations that describe the general motion of a continuous material in both Eulerian and Lagrangian forms which describe motion utilizing a general relationship between stress and strain for materials. We thus must introduce constitutive relationships (see Section 3) in order to quantify the material dependent relationship between stress and strain. A wide number of approaches to model these constitutive relationships have been developed and we focus much of our attention here on these. Once constitutive relationships are determined one can in principle solve the resulting set of motion equations with proper boundary and initial conditions. We conclude the paper in Section 4 by giving an example describing the motion of soil experiencing dynamic loading.

We remark that all of the considerations here are under isothermal conditions; in most physical problems where energy considerations (heat flow, temperature effects, entropy, etc.) are important, one may need to treat thermoelastic/thermoviscoelastic modeling. An introduction to this more challenging theory can be found in Chapter III of [16] and Chapter 5 of [30] with a more sophisticated thermodynamic treatment in [60]. We do not give details here since the subject is beyond the scope of our review.

2 Preliminary notions and balance laws

Throughout this review, bold letters are used to denote vectors unless otherwise indicated, $|\cdot|$ is used to denote the determinant of a matrix, and δ_{ij} denotes the Kronecker delta, that is, $\delta_{ij}=1$ for $i=j$ and zero otherwise. For convenience of presentation, we may occasionally use the Einstein notational convention (or index convention), where the convention is as follows: the repetition of an index in a term will denote a summation with respect to that index over its range. For example, the Einstein representations for $\sum_k \sum_l C_{ijkl}\varepsilon_{kl}$ and $\sum_i \sum_j \delta_{ij} dx_i dx_j$ are given by $C_{ijkl}\varepsilon_{kl}$ and $\delta_{ij}dx_i dx_j$, respectively. In the Cartesian coordinate system we may denote coordinate axes by x, y, and z or by x_1, x_2 and x_3, depending again on the ease of presentation. Accordingly, the components of a tensor σ are denoted by σ_{xx}, σ_{xy}, σ_{xz}, etc., in reference to coordinates x, y and z, and are denoted by σ_{ij}, $i,j=1,2,3$ in reference to coordinates x_1, x_2 and x_3.

In this section we first introduce some basic terminology and relationships used in continuum mechanics and then give a review on some fundamental physical laws such as the conservation of mass, and equation of motions in both Lagrangian and Eulerian forms. The content of this section is a summary of material from several popular mechanics books including [24, 26, 39, 44].

2.1 Preliminaries

2.1.1 Kinematics: deformation and motion

An external force applied to an object results in a displacement, and the displacement of a body generally has two components:

1. A rigid-body displacement: in this case the relative displacement between particles is zero, i.e., the shape and size of the body does not change.

2. A deformation: here there is a relative displacement between particles, i.e, the shape and/or the size are changed. There are two formulations describing deformation:

i. **Finite strain theory** which deals with deformations in which both rotations and strains are arbitrarily large. For example, elastomers, plastically-deforming materials and other fluids and biological soft tissue often undergo large deformations and may also require viscoelastic ideas and formulations.

ii. **Infinitesimal strain theory** which treats infinitesimal deformations of a continuum body. Many materials found in mechanical and civil engineering applications, such as concrete and steel, typically undergo small deformations.

For this presentation, we shall focus on deformations. When analyzing the deformation or motion of solids, or the flow of fluids, it is traditional (and helpful) to describe the sequence or evolution of configurations throughout time. One description for motion is made in terms of the material or fixed referential coordinates, and is called a material description or the *Lagrangian description*. The other description for motion is made in terms of the spatial or current coordinates, called a spatial description or *Eulerian description*. An intuitive comparison of these two descriptions would be that in the Eulerian description one places the coordinate or reference system for motion of an object on the object as it moves through a moving fluid (e.g., on a boat in a river) while in the Lagrangian description one observes and describes the motion of the object from a fixed vantage point (e.g., motion of the boat from a fixed point on a bridge over the river or on the side of the river.).

Lagrangian description

In a Lagrangian description an observer standing in the referential frame observes the changes in the position and physical properties as the material particles move in space as time progresses. In other words, this formulation focuses on individual particles as they move through space and time. *This description is normally used in solid mechanics*. In the Lagrangian description, the motion of a continuum is expressed by the mapping function $\mathbf{h}$ given by

$$\mathbf{x} = \mathbf{h}(\mathbf{X}, t), \tag{2.1}$$

which is a mapping from initial (undeformed/material) configuration Ω_0 to the present (deformed/spatial) configuration Ω_t. Hence, in a Lagrangian coordinate system the velocity of a particle at $\mathbf{X}$ at time t is given by

$$\mathbf{V}(\mathbf{X}, t) = \frac{\partial \mathbf{x}}{\partial t} = \frac{\partial \mathbf{h}(\mathbf{X}, t)}{\partial t},$$

and the total derivative (or material derivative) of a function $\psi(\mathbf{X}, t)$, which is denoted by a dot or the symbol D/Dt, is just the partial derivative of ψ with respect to t,

$$\frac{D}{Dt}\psi(\mathbf{X}, t) = \frac{\partial}{\partial t}\psi(\mathbf{X}, t).$$

Eulerian description

An Eulerian description focuses on the current configuration Ω_t, giving attention to what is occurring at a moving material point in space as time progresses. The coordinate system is relative to a moving point in the body and hence is a moving coordinate system. *This approach is often applied in the study of fluid mechanics*. Mathematically, the motion of a continuum using the Eulerian description is expressed by the mapping function

$$\mathbf{X} = \mathbf{h}^{-1}(\mathbf{x}, t),$$

which provides a tracing of the particle which now occupies the position $\mathbf{x}$ in the current configuration Ω_t from its original position $\mathbf{X}$ in the initial configuration Ω_0. The velocity of a particle at $\mathbf{x}$ at time t in the Eulerian coordinate system is

$$\mathbf{v}(\mathbf{x}, t) = \mathbf{V}\big(\mathbf{h}^{-1}(\mathbf{x}, t), t\big).$$

Hence, in an Eulerian coordinate system the total derivative (or material derivative) of a function $\psi(\mathbf{x}, t)$ is given by

$$\frac{D}{Dt}\psi(\mathbf{x}, t) = \frac{\partial}{\partial t}\psi(\mathbf{x}, t) + \sum_{i=1}^{3} v_i \frac{\partial}{\partial x_i}\psi(\mathbf{x}, t) = \frac{\partial}{\partial t}\psi(\mathbf{x}, t) + \mathbf{v}(\mathbf{x}, t) \cdot \nabla\psi(\mathbf{x}, t).$$

Remark 2.1. There are a number of the different names often used in the literature to refer to Lagrangian and Eulerian configurations. Synonymous terminology includes initial/referential, material, undeformed, fixed coordinates for Lagrangian and current/present, space, deformed, moving coordinates for Eulerian reference frames.

2.1.2 Displacement and strain

A particle P located originally at the coordinate $\mathbf{X} = (X_1, X_2, X_3)^T$ is moved to a place P' with coordinate $\mathbf{x} = (x_1, x_2, x_3)^T$ when the body moves and deforms. Then the vector $\mathbf{PP'}$, is called the *displacement or deformation vector* of the particle. The displacement vector is

$$\mathbf{x} - \mathbf{X}. \tag{2.2}$$

Let the variable $\mathbf{X} = (X_1, X_2, X_3)^T$ identify a particle in the original configuration of the body, and $\mathbf{x} = (x_1, x_2, x_3)^T$ be the coordinates of that particle when the body is deformed. Then the deformation of a body is known if x_1, x_2 and x_3 are known functions of X_1, X_2, X_3:

$$x_i = x_i(X_1, X_2, X_3), \qquad i = 1, 2, 3.$$

The (Lagrangian) displacement of the particle relative to $\mathbf{X}$ is given by

$$\mathbf{U}(\mathbf{X}) = \mathbf{x}(\mathbf{X}) - \mathbf{X}. \tag{2.3}$$

If we assume the transformation has a unique inverse, then we have

$$X_i = X_i(x_1, x_2, x_3), \quad i = 1, 2, 3,$$

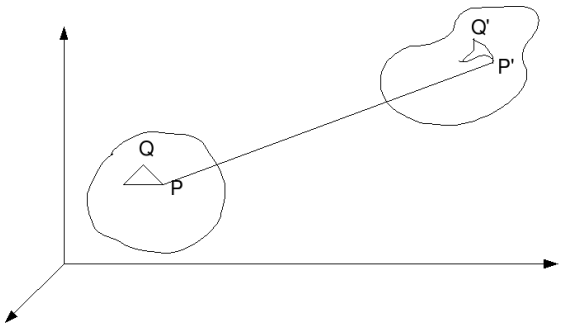

Figure 1: Deformation of a body.

for every particle in the body. Thus the (Eulerian) displacement of the particle relative to $\mathbf{x}$ is given by

$$\mathbf{u}(\mathbf{x}) = \mathbf{x} - \mathbf{X}(\mathbf{x}). \tag{2.4}$$

To relate deformation with stress, we must consider the stretching and distortion of the body. For this purpose, it is sufficient if we know the change of distance between any arbitrary pair of points.

Consider an infinitesimal line segment connecting the point $P(X_1, X_2, X_3)$ to a neighboring point $Q(X_1 + dX_1, X_2 + dX_2, X_3 + dX_3)$ (see Fig. 1). The square of the length of PQ in the original configuration is given by

$$|d\mathbf{X}|^2 = (d\mathbf{X})^T d\mathbf{X} = (dX_1)^2 + (dX_2)^2 + (dX_3)^2.$$

When P and Q are deformed to the points $P'(x_1, x_2, x_3)$ and $Q'(x_1 + dx_1, x_2 + dx_2, x_3 + dx_3)$, respectively, the square of length of $P'Q'$ is

$$|d\mathbf{x}|^2 = (d\mathbf{x})^T d\mathbf{x} = (dx_1)^2 + (dx_2)^2 + (dx_3)^2.$$

Definition 2.2. *The configuration gradient (often, in something of a misnomer, referred to as deformation gradient in the literature) is defined by*

$$A = \frac{d\mathbf{x}}{d\mathbf{X}} = \begin{bmatrix} \frac{\partial x_1}{\partial X_1} & \frac{\partial x_1}{\partial X_2} & \frac{\partial x_1}{\partial X_3} \\ \frac{\partial x_2}{\partial X_1} & \frac{\partial x_2}{\partial X_2} & \frac{\partial x_2}{\partial X_3} \\ \frac{\partial x_3}{\partial X_1} & \frac{\partial x_3}{\partial X_2} & \frac{\partial x_3}{\partial X_3} \end{bmatrix}. \tag{2.5}$$

The Lagrangian strain tensor

The Lagrangian strain tensor is measured with respect to the initial configuration (i.e., Lagrangian description). By the definition of configuration gradient, we have $d\mathbf{x} = Ad\mathbf{X}$ and

$$\begin{aligned} |d\mathbf{x}|^2 - |d\mathbf{X}|^2 =& (d\mathbf{x})^T d\mathbf{x} - (d\mathbf{X})^T d\mathbf{X} \\ =& (d\mathbf{X})^T A^T A d\mathbf{X} - (d\mathbf{X})^T d\mathbf{X} \\ =& (d\mathbf{X})^T (A^T A - I) d\mathbf{X}. \end{aligned}$$

The *Lagrangian (finite) strain tensor* **E** is defined by

$$\mathbf{E} = \frac{1}{2}(A^T A - I). \tag{2.6}$$

The strain tensor **E** was introduced by Green and St. Venant. Accordingly, in the literature **E** is often called the *Green's strain tensor* or the *Green-St. Venant strain tensor*. In addition, from (2.6) we see that the Lagrangian strain tensor **E** is symmetric.

If the strain satisfies $A^T A - I = 0$, then we say the object is undeformed; otherwise, it is deformed. We next explore the relationship between the displacement and strain. By (2.3) and (2.5) we have the true *deformation gradient* given by

$$\nabla \mathbf{U} = \begin{bmatrix} \frac{\partial x_1}{\partial X_1} - 1 & \frac{\partial x_1}{\partial X_2} & \frac{\partial x_1}{\partial X_3} \\ \frac{\partial x_2}{\partial X_1} & \frac{\partial x_2}{\partial X_2} - 1 & \frac{\partial x_2}{\partial X_3} \\ \frac{\partial x_3}{\partial X_1} & \frac{\partial x_3}{\partial X_2} & \frac{\partial x_3}{\partial X_3} - 1 \end{bmatrix} = A - I,$$

or

$$\frac{\partial U_i}{\partial X_j} = \frac{\partial x_i}{\partial X_j} - \delta_{ij}, \quad j = 1,2,3, \;\; i = 1,2,3,$$

where I is the identity matrix, and $\mathbf{U} = (U_1, U_2, U_3)^T$. Thus, because

$$A = \nabla \mathbf{U} + I,$$

the relationship between Lagrangian strain (2.6) and displacement is given by

$$E_{ij} = \frac{1}{2}\Big[\frac{\partial U_i}{\partial X_j} + \frac{\partial U_j}{\partial X_i} + \frac{\partial U_k}{\partial X_i}\frac{\partial U_k}{\partial X_j}\Big],$$

where E_{ij} is the (i,j) component of strain tensor **E**.

The Eulerian strain tensor

The Eulerian strain tensor is measured with respect to the deformed or current configuration (i.e., Eulerian description). By using $d\mathbf{X} = A^{-1}d\mathbf{x}$, we find

$$\begin{aligned} |d\mathbf{x}|^2 - |d\mathbf{X}|^2 =& (d\mathbf{x})^T d\mathbf{x} - (d\mathbf{x})^T (A^{-1})^T A^{-1} d\mathbf{x} \\ =& (d\mathbf{x})^T (I - (A^{-1})^T A^{-1}) d\mathbf{x}, \end{aligned}$$

and the *Eulerian (finite) strain tensor* **e** is defined by

$$\mathbf{e} = \frac{1}{2}\big(I - (A^{-1})^T A^{-1}\big). \tag{2.7}$$

The strain tensor **e** was introduced by Cauchy for infinitesimal strains and by Almansi and Hamel for finite strains; **e** is also known as *Almansi's strain* in the literature. In addition, we observe from (2.7) that Eulerian strain tensor **e** is also symmetric.

We also may give the relationship between the displacement and strain in the Eulerian formulation. By (2.4) and (2.5) we have

$$\nabla \mathbf{u} = \begin{bmatrix} 1-\frac{\partial X_1}{\partial x_1} & -\frac{\partial X_1}{\partial x_2} & -\frac{\partial X_1}{\partial x_3} \\ -\frac{\partial X_2}{\partial x_1} & 1-\frac{\partial X_2}{\partial x_2} & -\frac{\partial X_2}{\partial x_3} \\ -\frac{\partial X_3}{\partial x_1} & -\frac{\partial X_3}{\partial x_2} & 1-\frac{\partial X_3}{\partial x_3} \end{bmatrix} = I - A^{-1},$$

or

$$\frac{\partial u_i}{\partial x_j} = \delta_{ij} - \frac{\partial X_i}{\partial x_j}, \quad j = 1,2,3, \;\; i = 1,2,3,$$

where $\mathbf{u} = (u_1, u_2, u_3)^T$. Thus, the relationship between Eulerian strain and displacement is given by

$$e_{ij} = \frac{1}{2}\Big[\frac{\partial u_i}{\partial x_j} + \frac{\partial u_j}{\partial x_i} - \frac{\partial u_k}{\partial x_i}\frac{\partial u_k}{\partial x_j}\Big],$$

where e_{ij} is the (i,j) component of strain tensor $\mathbf{e}$.

Remark 2.3. There are two tensors that are often encountered in the finite strain theory. One is the *right Cauchy-Green configuration (deformation) tensor*, which is defined by

$$D_R = A^T A = \Big(\frac{\partial x_k}{\partial X_i}\frac{\partial x_k}{\partial X_j}\Big),$$

and the other is the *left Cauchy-Green configuration (deformation) tensor* defined by

$$D_L = AA^T = \Big(\frac{\partial x_i}{\partial X_k}\frac{\partial x_j}{\partial X_k}\Big).$$

The inverse of D_L is called the *Finger deformation tensor*. Invariants of D_R and D_L are often used in the expressions for *strain energy density functions* (to be discussed below in Section 3.1.2). The most commonly used invariants are defined to be the coefficients of their characteristic equations. For example, frequently encountered invariants of D_R are defined by

$$\begin{aligned} I_1 &= \mathrm{tr}(D_R) = \lambda_1^2 + \lambda_2^2 + \lambda_3^2, \\ I_2 &= \frac{1}{2}\big[\mathrm{tr}(D_R^2) - (\mathrm{tr}(D_R))^2\big] = \lambda_1^2\lambda_2^2 + \lambda_2^2\lambda_3^2 + \lambda_3^2\lambda_1^2, \\ I_3 &= \det(D_R) = \lambda_1^2\lambda_2^2\lambda_3^2, \end{aligned}$$

where λ_i, $i = 1,2,3$ are the eigenvalues of A, and also known as *principal stretches* (these will be discussed later in Section 3.1.2).

Infinitesimal strain theory

Infinitesimal strain theory is also called *small deformation theory*, *small displacement theory* or *small displacement-gradient theory*. In infinitesimal strain theory, it is assumed that the components of displacement u_i are such that their first derivatives are so small that higher order terms such as the squares and the products of the partial derivatives of u_i are negligible compared with the first-order terms. In this case e_{ij} reduces to Cauchy's *infinitesimal strain tensor*

$$\varepsilon_{ij} = \frac{1}{2}\Big[\frac{\partial u_i}{\partial x_j} + \frac{\partial u_j}{\partial x_i}\Big], \tag{2.8}$$

(hence the infinitesimal strain tensor is also symmetric). Thus, $\varepsilon_{ij} = \varepsilon_{ji}$. We note that in this case the distinction between the Lagrangian and Eulerian strain tensors disappears (i.e., $E_{ij} \approx e_{ij} \approx \varepsilon_{ij}$), since it is immaterial whether the derivatives of the displacement are calculated at the position of a point before or after deformation. Hence, the necessity of specifying whether the strains are measured with respect to the initial configuration (Lagrangian description) or with respect to the deformed configuration (Eulerian description) is characteristic of a finite strain analysis and the two different formulations are typically not encountered in the infinitesimal theory.

2.1.3 Stress

Stress is a measure of the average amount of force exerted per unit area (in units $\mathrm{N/m^2}$ or Pa), and it is a reaction to external forces on a surface of a body. Stress was introduced into the theory of elasticity by Cauchy almost two hundred years ago.

Definition 2.4. *The stress vector (traction) is defined by*

$$\mathbf{T}^{(\mathbf{n})} = \frac{d\mathbf{F}}{d\Gamma} = \lim_{\Delta\Gamma\to 0}\frac{\Delta\mathbf{F}}{\Delta\Gamma},$$

where the superscript $(\mathbf{n})$ *is introduced to denote the direction of the normal vector* $\mathbf{n}$ *of the surface* Γ *and* $\mathbf{F}$ *is the force on the surface.*

To further elaborate on this concept, consider a small cube in the body as depicted in Fig. 2 (left). Let the surface of the cube normal (perpendicular) to the axis z be donated by $\nabla\Gamma_z$. Let the stress vector that acts on the surface $\nabla\Gamma_z$ be $\mathbf{T}^{(\mathbf{e}_3)}$, where $\mathbf{e}_3 = (0,0,1)^T$. Resolve $\mathbf{T}^{(\mathbf{e}_3)}$ into three components in the direction of the coordinate axes and denote them by σ_{zx}, σ_{zy} and σ_{zz}. Similarly we may consider surface $\nabla\Gamma_x$ and $\nabla\Gamma_y$ perpendicular to x and y, the stress vectors acting on them, and their components in the x, y and z directions. The components σ_{xx}, σ_{yy} and σ_{zz} are called normal stresses, and σ_{xy}, σ_{xz}, σ_{yx}, σ_{yz}, σ_{zx} and σ_{zy} are called shear stresses. *A stress component is positive if it acts in the positive direction of the coordinate axes*. We remark that the notation $\sigma_{\text{face, direction}}$ is consistently used in elasticity theory.

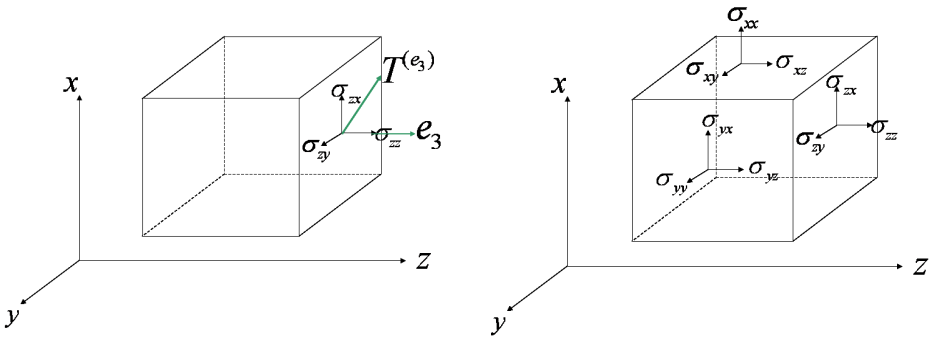

Figure 2: Notations of stress components.

Definition 2.5. *The* Cauchy stress tensor *is defined by*

$$\sigma = \left[\begin{array}{ccc} \mathbf{T}^{(\mathbf{e}_1)} & \mathbf{T}^{(\mathbf{e}_2)} & \mathbf{T}^{(\mathbf{e}_3)} \end{array} \right] = \left[\begin{array}{ccc} \sigma_{xx} & \sigma_{yx} & \sigma_{zx} \\ \sigma_{xy} & \sigma_{yy} & \sigma_{zy} \\ \sigma_{xz} & \sigma_{yz} & \sigma_{zz} \end{array} \right], \tag{2.9}$$

where

$$\mathbf{e}_1 = (1,0,0)^T, \quad \mathbf{e}_2 = (0,1,0)^T, \quad \textit{and} \quad \mathbf{e}_3 = (0,0,1)^T.$$

We have the following basic formulation due to Cauchy.

Theorem 2.6. *(see* [25, pp.69]*) Let* $\mathbf{T}^{(\mathbf{n})}$ *be the stress vector acting on* $d\Gamma$ *whose outer normal vector is* $\mathbf{n}$*, as illustrated in Fig.* 3*. Cauchy's formula expresses* $\mathbf{T}^{(\mathbf{n})}$ *as a function of the stress vectors on the planes perpendicular to the coordinate axes, i.e., in terms of the components of the Cauchy stress tensor. This formula asserts that*

$$T_x^{(\mathbf{n})} = \sigma_{xx} n_x + \sigma_{yx} n_y + \sigma_{zx} n_z, \tag{2.10a}$$

$$T_y^{(\mathbf{n})} = \sigma_{xy} n_x + \sigma_{yy} n_y + \sigma_{zy} n_z, \tag{2.10b}$$

$$T_z^{(\mathbf{n})} = \sigma_{xz} n_x + \sigma_{yz} n_y + \sigma_{zz} n_z. \tag{2.10c}$$

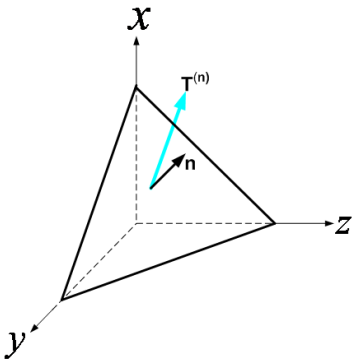

Figure 3: Stress vector acting on a plane with normal $\mathbf{n}$.

Here

$$\mathbf{T}^{(\mathbf{n})} = \left(T_x^{(\mathbf{n})}, T_y^{(\mathbf{n})}, T_z^{(\mathbf{n})}\right)^T, \quad \textit{and} \quad \mathbf{n} = (n_x, n_y, n_z)^T.$$

Cauchy's formula (2.10) *can be written concisely as*

$$\mathbf{T}^{(\mathbf{n})} = \sigma\mathbf{n},$$

where σ is the Cauchy stress tensor defined in (2.9).

Remark 2.7. In addition to the Cauchy stress tensor, there are other stress tensors encountered in practice, such as the *first Piola-Kirchhoff stress tensor* and *second Piola-Kirchhoff stress tensor*. The differences between the Cauchy stress tensor and the Piola-Kirchhoff stress tensors as well as relationships between the tensors can be illustrated as follows:
1. Cauchy stress tensor: relates forces in the present (deformed/spatial) configuration to areas in the present configuration. Hence, sometimes the Cauchy stress is also called the *true stress*. In addition, the Cauchy stress tensor is symmetric, which is implied by the fact that the equilibrium of an element requires that the resultant moments vanish. We will see in Section 2.2.4 that the Cauchy stress tensor is used in the Eulerian equation of motion. Hence the Cauchy stress tensor is also referred to as the Eulerian stress tensor.
2. First Piola-Kirchhoff stress tensor (also called the *Lagrangian stress tensor* in [24,25]): relates forces in the present configuration with areas in the initial configuration. The relationship between the first Piola-Kirchhoff stress tensor $\mathbf{P}$ and the Cauchy stress tensor σ is given by

$$\mathbf{P} = |A|\sigma(A^{-1})^T. \tag{2.11}$$

From the above equation, we see that in general the first Piola-Kirchhoff stress tensor is not symmetric (its transpose is called the *nominal stress tensor* or *engineering stress tensor*). Hence, the first Piola-Kirchhoff stress tensor will be inconvenient to use in a stress-strain law in which the strain tensor is always symmetric. In addition, we will see in Section 2.2.5 that the first Piola-Kirchhoff stress tensor is used in the Lagrangian equation of motion. As pointed out in [25], the first Piola-Kirchhoff stress tensor is the most convenient for the reduction of laboratory experimental data.
3. Second Piola-Kirchhoff stress tensor (referred to as *Kirchoff stress tensor* in [24,25], though in some references such as [44] Kirchhoff stress tensor refers to a weighted Cauchy stress tensor and is defined by $|A|\sigma$): relates forces in the initial configuration to areas in the initial configuration. The relationship between the second Piola-Kirchhoff stress tensor $\mathbf{S}$ and the Cauchy stress tensor σ is given by

$$\mathbf{S} = |A|A^{-1}\sigma(A^{-1})^T. \tag{2.12}$$

From the above formula we see that the second Piola-Kirchhoff stress tensor is symmetric. Hence, the second Piola-Kirchhoff stress tensor is more suitable than the first Piola-Kirchhoff stress tensor to use in a stress-strain law. In addition, by (2.11) and (2.12) we find that

$$\mathbf{S} = A^{-1}\mathbf{P}. \tag{2.13}$$

Note that for infinitesimal deformations, the Cauchy stress tensor, the first Piola-Kirchhoff stress tensor and the second Piola-Kirchhoff tensor are identical. Hence, it is necessary only in finite strain theory to specify whether the stresses are measured with respect to the initial configuration (Lagrangian description) or with respect to the deformed configuration (Eulerian description).

2.2 Equations of motion of a continuum

There are two common approaches in the literature to derive the equation of motion of a continuum: the differential equation approach (for example, in [26]) and the integral approach (for example, in [26,44]). In this section, we will use an integral approach to derive the equation of continuity and the equation of motion of a continuum, first in the *Eulerian (or moving) coordinate system* and then in the *Lagrangian coordinate system*. In the following, we will sometimes use Ω to denote Ω_t, and Γ to denote Γ_t for ease in the presentation; these will refer to volume or surface elements, respectively, that are time dependent.

Before deriving the equations of motion of a continuum, we first discuss forces. There are two types of external forces acting on material bodies in the mechanics of continuum media:

1. Body forces (N/m^3), acting on elements of volume of body. For example, gravitational forces and electromagnetic forces are body forces.

2. Surface forces (N/m^2), or stress, acting on surface elements. For example, aerodynamics pressure acting on a body, stress between one part of a body on another, etc., are surface forces.

Then the total force $\mathbf{F}$ acting upon the material occupying the region Ω interior to a closed surface Γ is

$$\mathbf{F} = \oint_{\Gamma} \mathbf{T}^{(\mathbf{n})} d\Gamma + \int_{\Omega} \mathbf{f} d\Omega, \tag{2.14}$$

where $\mathbf{f} = (f_x, f_y, f_z)^T$ is the body force, and $\mathbf{T}^{(\mathbf{n})}$ is the stress vector acting on $d\Gamma$ whose outer normal vector is $\mathbf{n}$.

The expression (2.14) is a universal force balance statement independent of any particular coordinate system being used. Of course, with either the Eulerian or Lagrangian formulation, the stresses and forces must be expressed in terms of the appropriate coordinate system.

2.2.1 The material derivative of a volume integral

To carry out our derivations, we need a calculus for interchanging integration and differentiation when both the limits of the integration and the integrand depend on the differentiation variable. Let $\Phi(t)$ be a volume integral of a continuously differential function $\phi(x,y,z,t)$ defined over a spatial domain Ω_t occupied by a given set of material particles at time t, i.e.,

$$\Phi(t) = \iiint_{\Omega_t} \phi(x,y,z,t) dxdydz.$$

Then the rate of change of $\Phi(t)$ with respect to t is given by (suppressing the multiple integral notation here and below when it is clearly understood that the integral is a volume or surface integral)

$$\frac{d\Phi}{dt} = \int_{\Omega_t} \frac{\partial \phi}{\partial t} d\Omega + \int_{\Gamma_t} (\phi v_x n_x + \phi v_y n_y + \phi v_z n_z) d\Gamma, \tag{2.15}$$

where on the boundary Γ_t of Ω_t, $\mathbf{v} = \mathbf{v}(t)$ is the velocity

$$\mathbf{v}(t) = \left(\frac{dx}{dt}, \frac{dy}{dt}, \frac{dz}{dt}\right)^T.$$

Eq. (2.15) can be written concisely as

$$\frac{d\Phi}{dt} = \int_{\Omega_t} \frac{\partial \phi}{\partial t} d\Omega + \int_{\Gamma_t} \phi \mathbf{v} \cdot \mathbf{n} d\Gamma.$$

The first term on the right side corresponds to rate of change in a fixed volume, and the second term corresponds to the convective transfer through the surface. By Gauss' theorem, Eq. (2.15) can also be written as

$$\frac{d\Phi}{dt} = \int_{\Omega_t} \left(\frac{\partial \phi}{\partial t} + \frac{\partial \phi v_x}{\partial x} + \frac{\partial \phi v_y}{\partial y} + \frac{\partial \phi v_z}{\partial z}\right) d\Omega, \tag{2.16}$$

or more concisely as

$$\frac{d\Phi}{dt} = \int_{\Omega_t} \left(\frac{\partial \phi}{\partial t} + \nabla \cdot (\phi \mathbf{v})\right) d\Omega.$$

This rate, called the *material derivative* of Φ, is defined for a given set of material particles in a moving volume. We note that when $\Omega_t = \Omega_0$ for all t (i.e., the boundary Γ is not moving so that $\mathbf{v} = \mathbf{0}$), this becomes simply

$$\frac{d}{dt} \int_{\Omega_0} \phi(x, y, z, t) dx dy dz = \int_{\Omega_0} \frac{\partial \phi}{\partial t}(x, y, z, t) dx dy dz.$$

2.2.2 The equation of continuity

We next derive the equation of continuity for an arbitrary mass of particles that may be changing in time. The mass contained in a domain Ω_t at time t is

$$m(t) = \int_{\Omega_t} \rho(x, y, z, t) dx dy dz.$$

Conservation of mass requires that $dm/dt = 0$ and thus we have from (2.16)

$$\frac{dm}{dt} = \int_{\Omega_t} \left[\frac{\partial \rho}{\partial t} + \frac{\partial \rho v_x}{\partial x} + \frac{\partial \rho v_y}{\partial y} + \frac{\partial \rho v_z}{\partial z}\right] d\Omega.$$

Hence, we obtain

$$\int_{\Omega_t} \left[\frac{\partial \rho}{\partial t} + \frac{\partial \rho v_x}{\partial x} + \frac{\partial \rho v_y}{\partial y} + \frac{\partial \rho v_z}{\partial z}\right] d\Omega = 0.$$

Since the above equality holds for an arbitrary domain Ω_t, we obtain the pointwise *equation of continuity*

$$\frac{\partial \rho}{\partial t} + \frac{\partial \rho v_x}{\partial x} + \frac{\partial \rho v_y}{\partial y} + \frac{\partial \rho v_z}{\partial z} = 0, \tag{2.17}$$

which can be written concisely as

$$\frac{\partial \rho}{\partial t} + \nabla \cdot (\rho \mathbf{v}) = 0.$$

2.2.3 The Reynolds transport theorem

In this subsection, we will use the material derivative (2.16) as well as the equation of continuity (2.17) to derive the celebrated *Reynolds transport theorem*. By (2.16) we find that

$$\frac{d}{dt}\int_{\Omega_t} \rho v_z d\Omega = \int_{\Omega_t} \Big(\frac{\partial (\rho v_z)}{\partial t} + \frac{\partial \rho v_z v_x}{\partial x} + \frac{\partial \rho v_z v_y}{\partial y} + \frac{\partial \rho v_z v_z}{\partial z} \Big) d\Omega.$$

Then using the equation of continuity (2.17), we find that the integrand of the right side of the above equation is equal to

$$\begin{aligned}
&\frac{\partial \rho}{\partial t} v_z + \rho \frac{\partial v_z}{\partial t} + v_z \Big(\frac{\partial \rho v_x}{\partial x} + \frac{\partial \rho v_y}{\partial y} + \frac{\partial \rho v_z}{\partial z} \Big) + \rho v_x \frac{\partial v_z}{\partial x} + \rho v_y \frac{\partial v_z}{\partial y} + \rho v_z \frac{\partial v_z}{\partial z} \\
=& v_z \Big(\frac{\partial \rho}{\partial t} + \frac{\partial \rho v_x}{\partial x} + \frac{\partial \rho v_y}{\partial y} + \frac{\partial \rho v_z}{\partial z} \Big) + \rho \Big(\frac{\partial v_z}{\partial t} + v_x \frac{\partial v_z}{\partial x} + v_y \frac{\partial v_z}{\partial y} + v_z \frac{\partial v_z}{\partial z} \Big) \\
=& \rho \Big(\frac{\partial v_z}{\partial t} + v_x \frac{\partial v_z}{\partial x} + v_y \frac{\partial v_z}{\partial y} + v_z \frac{\partial v_z}{\partial z} \Big).
\end{aligned}$$

Hence, we have

$$\frac{d}{dt}\int_{\Omega_t} \rho v_z d\Omega = \int_{\Omega_t} \rho \Big(\frac{\partial v_z}{\partial t} + v_x \frac{\partial v_z}{\partial x} + v_y \frac{\partial v_z}{\partial y} + v_z \frac{\partial v_z}{\partial z} \Big) d\Omega. \tag{2.18}$$

Eq. (2.18) is the Reynolds transport theorem, which is usually written concisely as

$$\frac{d}{dt}\int_{\Omega_t} \rho v_z d\Omega = \int_{\Omega_t} \rho \frac{Dv_z}{Dt} d\Omega,$$

where Dv_z/Dt is the total derivative of v_z, and is given by

$$\frac{D}{Dt} v_z(x,y,z,t) = \frac{\partial v_z}{\partial t} + v_x \frac{\partial v_z}{\partial x} + v_y \frac{\partial v_z}{\partial y} + v_z \frac{\partial v_z}{\partial z}.$$

We note that the above is independent of any coordinate system and depends only on the rules of calculus and the assumptions of continuity of mass in a time dependent volume of particles.

2.2.4 The Eulerian equations of motion of a continuum

We are now ready to use the above rules of calculus and the continuity of mass as embodied in the Reynolds transport theorem to derive the equations of motion in an Eulerian coordinate system. Throughout we have $\Omega = \Omega_t$ and $\Gamma = \Gamma_t$ (we will suppress the subscripts) and we assume the coordinate system (x, y, z) is now moving (changing with the volume element) with a velocity $\mathbf{v} = (dx/dt, dy/dt, dz/dt)^T$ of the deformation of the material. The resultant force F_z in the z-direction on an arbitrary volume Ω is

$$F_z = \int_\Gamma T_z^{(\mathbf{n})} d\Gamma + \int_\Omega f_z d\Omega. \tag{2.19}$$

By Cauchy's formula (2.10) and Gauss' theorem we have

$$\begin{aligned}\int_\Gamma T_z^{(\mathbf{n})} d\Gamma &= \int_\Gamma \Big(\sigma_{xz} n_x + \sigma_{yz} n_y + \sigma_{zz} n_z\Big) d\Gamma \\ &= \int_\Omega \Big(\frac{\partial \sigma_{xz}}{\partial x} + \frac{\partial \sigma_{yz}}{\partial y} + \frac{\partial \sigma_{zz}}{\partial z}\Big) d\Omega.\end{aligned}$$

Hence, by the above equality and (2.19), we obtain

$$F_z = \int_\Omega \Big(\frac{\partial \sigma_{xz}}{\partial x} + \frac{\partial \sigma_{yz}}{\partial y} + \frac{\partial \sigma_{zz}}{\partial z} + f_z\Big) d\Omega.$$

Newton's law states that

$$\frac{d}{dt}\int_\Omega \rho v_z d\Omega = \int_\Omega \Big(\frac{\partial \sigma_{xz}}{\partial x} + \frac{\partial \sigma_{yz}}{\partial y} + \frac{\partial \sigma_{zz}}{\partial z} + f_z\Big) d\Omega.$$

Hence, by the Reynolds transport theorem we have

$$\int_\Omega \rho\Big(\frac{\partial v_z}{\partial t} + v_x\frac{\partial v_z}{\partial x} + v_y\frac{\partial v_z}{\partial y} + v_z\frac{\partial v_z}{\partial z}\Big) d\Omega = \int_\Omega \Big(\frac{\partial \sigma_{xz}}{\partial x} + \frac{\partial \sigma_{yz}}{\partial y} + \frac{\partial \sigma_{zz}}{\partial z} + f_z\Big) d\Omega.$$

Note that because the above equality holds for an arbitrary domain Ω, the integrands on both sides must be equal. Thus, we have

$$\rho\Big(\frac{\partial v_z}{\partial t} + v_x\frac{\partial v_z}{\partial x} + v_y\frac{\partial v_z}{\partial y} + v_z\frac{\partial v_z}{\partial z}\Big) = \frac{\partial \sigma_{xz}}{\partial x} + \frac{\partial \sigma_{yz}}{\partial y} + \frac{\partial \sigma_{zz}}{\partial z} + f_z,$$

or written concisely as

$$\rho\frac{Dv_z}{Dt} = \nabla \cdot \sigma_{\bullet,z} + f_z,$$

which is the *equation of motion of a continuum* in the z-direction. The entire set for *the equations of motion of a continuum in an Eulerian coordinate system* is given as follows:

$$\rho\Big(\frac{\partial v_x}{\partial t} + v_x\frac{\partial v_x}{\partial x} + v_y\frac{\partial v_x}{\partial y} + v_z\frac{\partial v_x}{\partial z}\Big) = \frac{\partial \sigma_{xx}}{\partial x} + \frac{\partial \sigma_{yx}}{\partial y} + \frac{\partial \sigma_{zx}}{\partial z} + f_x, \tag{2.20a}$$

$$\rho\Big(\frac{\partial v_y}{\partial t} + v_x\frac{\partial v_y}{\partial x} + v_y\frac{\partial v_y}{\partial y} + v_z\frac{\partial v_y}{\partial z}\Big) = \frac{\partial \sigma_{xy}}{\partial x} + \frac{\partial \sigma_{yy}}{\partial y} + \frac{\partial \sigma_{zy}}{\partial z} + f_y, \tag{2.20b}$$

$$\rho\Big(\frac{\partial v_z}{\partial t} + v_x\frac{\partial v_z}{\partial x} + v_y\frac{\partial v_z}{\partial y} + v_z\frac{\partial v_z}{\partial z}\Big) = \frac{\partial \sigma_{xz}}{\partial x} + \frac{\partial \sigma_{yz}}{\partial y} + \frac{\partial \sigma_{zz}}{\partial z} + f_z. \tag{2.20c}$$

We note that (2.20) is also called *Cauchy's equation of motion* or *Cauchy's momentum equation* in some literature. Eq. (2.20) can be written in vector form as

$$\rho\Big(\frac{\partial \mathbf{v}}{\partial t}+(\mathbf{v}\cdot\nabla)\mathbf{v}\Big)=\nabla\cdot\boldsymbol{\sigma}+\mathbf{f},$$

where $\boldsymbol{\sigma}$ is the Cauchy stress tensor defined in (2.9). It is often desirable to express these equations of motion in terms of displacements $\mathbf{u}$. We find (because the Eulerian velocity is given in terms of the displacement (2.4) by $\mathbf{v}=\partial\mathbf{u}/\partial t$)

$$\rho\Big[\frac{\partial^2\mathbf{u}}{\partial t^2}+\Big(\frac{\partial\mathbf{u}}{\partial t}\cdot\nabla\Big)\frac{\partial\mathbf{u}}{\partial t}\Big]=\nabla\cdot\boldsymbol{\sigma}+\mathbf{f}. \tag{2.21}$$

2.2.5 The Lagrangian equations of motion of a continuum

Next we will rewrite (2.20) in terms of a Lagrangian description, that is, we will derive an equation of motion in the Lagrangian coordinate system (O-XYZ coordinate system). Let Γ_0 denote the boundary of Ω_0 in the initial (undeformed/material) configuration, and $\mathbf{n}_0$ be the outer normal vector on Γ_0. By Nanson's formula [44] we have

$$\mathbf{n}d\Gamma=|A|(A^{-1})^T\mathbf{n}_0d\Gamma_0, \tag{2.22}$$

where $\mathbf{n}_0=(n_{0X},n_{0Y},n_{0Z})^T$, A is the configuration gradient defined by (2.5). Multiplying both sides of (2.22) by $\boldsymbol{\sigma}$ we obtain

$$\boldsymbol{\sigma}\mathbf{n}d\Gamma=|A|\boldsymbol{\sigma}(A^{-1})^T\mathbf{n}_0d\Gamma_0.$$

By (2.11), we have

$$\boldsymbol{\sigma}\mathbf{n}d\Gamma=\mathbf{P}\mathbf{n}_0d\Gamma_0.$$

Let $\mathbf{f}_0$ be the external body force acting on Ω_0 ($\mathbf{f}_0=|A|\mathbf{f}$), let $\rho_0(X,Y,Z,t)$ be the material density in the Lagrangian coordinate system (conservation of mass implies that $\rho_0=|A|\rho$), and $V(X,Y,Z,t)$ be the velocity in the Lagrangian coordinate system. Then we can rewrite the resultant force in the z-direction in the Eulerian coordinate system as the resultant force in the Z direction in the Lagrangian coordinate system, which is

$$F_{0Z}=\int_{\Gamma_0}(P_{ZX}n_{0X}+P_{ZY}n_{0Y}+P_{ZZ}n_{0Z})d\Gamma_0+\int_{\Omega_0}f_{0Z}d\Omega_0.$$

Then by Gauss' Theorem and the above equation we find that

$$F_{0Z}=\int_{\Omega_0}\Big(\frac{\partial P_{ZX}}{\partial X}+\frac{\partial P_{ZY}}{\partial Y}+\frac{\partial P_{ZZ}}{\partial Z}\Big)d\Omega_0+\int_{\Omega_0}f_{0Z}d\Omega_0.$$

We can rewrite Reynolds transport theorem (2.18) in the Lagrangian coordinate system and find

$$\frac{d}{dt}\int_{\Omega}\rho v_zd\Omega=\int_{\Omega}\rho\frac{Dv_z}{Dt}d\Omega=\int_{\Omega_0}\rho_0\frac{DV_Z}{Dt}d\Omega_0.$$

Note that

$$\frac{DV_Z}{Dt} = \frac{\partial V_Z}{\partial t}.$$

Hence, we can rewrite Newton's law in the Lagrangian coordinate system as

$$\int_{\Omega_0} \rho_0 \frac{\partial V_Z}{\partial t} \Omega_0 = \int_{\Omega_0} \Big(\frac{\partial P_{ZX}}{\partial X} + \frac{\partial P_{ZY}}{\partial Y} + \frac{\partial P_{ZZ}}{\partial Z} + f_{0Z} \Big) d\Omega_0.$$

Note that the above equality holds for any Ω_0. Thus we have

$$\rho_0 \frac{\partial V_Z}{\partial t} = \frac{\partial P_{ZX}}{\partial X} + \frac{\partial P_{ZY}}{\partial Y} + \frac{\partial P_{ZZ}}{\partial Z} + f_{0Z},$$

which is the equation of motion in the Z-direction. Then *the equations of motion in the Lagrangian coordinate system* are given by

$$\rho_0 \frac{\partial V_X}{\partial t} = \frac{\partial P_{XX}}{\partial X} + \frac{\partial P_{XY}}{\partial Y} + \frac{\partial P_{XZ}}{\partial Z} + f_{0X}, \tag{2.23a}$$

$$\rho_0 \frac{\partial V_Y}{\partial t} = \frac{\partial P_{YX}}{\partial X} + \frac{\partial P_{YY}}{\partial Y} + \frac{\partial P_{YZ}}{\partial Z} + f_{0Y}, \tag{2.23b}$$

$$\rho_0 \frac{\partial V_Z}{\partial t} = \frac{\partial P_{ZX}}{\partial X} + \frac{\partial P_{ZY}}{\partial Y} + \frac{\partial P_{ZZ}}{\partial Z} + f_{0Z}, \tag{2.23c}$$

or, written concisely,

$$\rho_0 \frac{\partial \mathbf{V}}{\partial t} = \nabla \cdot \mathbf{P} + \mathbf{f}_0.$$

Note that

$$\mathbf{V} = \frac{\partial \mathbf{U}}{\partial t}.$$

Hence, the Lagrangian equations of motion in terms of displacement is given by

$$\rho_0 \frac{\partial^2 \mathbf{U}}{\partial t^2} = \nabla \cdot \mathbf{P} + \mathbf{f}_0. \tag{2.24}$$

Remark 2.8. We note that the equations of motion (2.21) in the Eulerian (or moving) coordinate system are inherently *nonlinear* independent of the constitutive law assumptions (discussed in the next section) we might subsequently adopt. On the other hand, the Lagrangian formulation (2.24) (relative to a fixed referential coordinate system) will yield a linear system if a linear constitutive law is assumed. Thus, there are obvious advantages to using the Lagrangian formulation in linear theory (i.e., when a linear constitutive law is assumed).

3 Constitutive relationships: stress and strain

In the preceding discussions, we have focused on relationships between displacements (and their rates) and the stress tensors. We have also related strain tensors

to displacements. To complete our derivations of the equations of motion, we must know (or assume) the relationships (constitutive "laws") between stress and strain. Constitutive laws are usually formulated based on empirical observations, and they "hold" for a given material and are thus material dependent. Moreover, they must be independent of any referential coordinate system that we choose. In addition, we must note that the constitutive law describes an ideal material, and it should provide a close approximation to the actual behavior of the real material that this constitutive law is intended to model.

The concept of *isotropy* is used frequently as a simplifying assumption in continuum mechanics, and many useful materials are indeed isotropic or approximately so. We proceed to present the formal definition of an isotropic tensor and isotropic materials.

Definition 3.1. *If a tensor has the same array of components when the frame of reference is rotated or reflected (i.e., invariance under rotation or reflection), then it is said to be an isotropic tensor. A material whose constitutive equation is isotropic is said to be an* isotropic material.

Remark 3.2. If the tensor $\mathcal{D}_{ijkl}$ is isotropic, then it can be expressed in terms of two independent constants ν and μ by

$$\mathcal{D}_{ijkl} = \nu\delta_{ij}\delta_{kl} + \mu(\delta_{ik}\delta_{jl} + \delta_{il}\delta_{jk}). \tag{3.1}$$

We note that here ν is a Lamé parameter not to be confused with the Poisson ratio also encountered in elasticity.

Since we are interested in incorporating the constitutive laws for stress and strain into the equations of motion, we will only present constitutive laws for their relaxation forms, i.e., stress is a function of strain and/or strain rate. The corresponding compliance forms, i.e., the strain in terms of stress and/or stress rate, for most of these constitutive laws can be defined similarly by just interchanging the role of stress and strain. For convenience, we will suppress the spatial dependence of both stress and strain when the constitutive relationship is given. Recall also that in an infinitesimal setting the stress tensors are all equivalent; unless noted otherwise, we will use σ to denote the stress in the following discussion and assume an infinitesimal setting. The rest of this section is outlined as follows: we first talk about the constitutive equations used in elastic materials in Section 3.1, and then we present and discuss a number of constitutive laws appearing in the literature for the viscoelastic materials in Section 3.2.

3.1 Elastic materials

Elasticity is the physical property of a material that when it deforms under stress (e.g., external forces), it returns to its original shape when the stress is removed. For an elastic material, the stress-strain curve is the same for the loading and unloading process, and the stress only depends on the current strain, not on its history. A familiar

example of an elastic material body is a typical metal spring. Below we will discuss linear elasticity in Section 3.1.1 and then follow with comments on nonlinear elasticity in Section 3.1.2.

3.1.1 Linear elasticity

The classical theory of elasticity deals with the mechanical properties of elastic solids for which the stress is directly proportional to the stress in small deformations. Most structural metals are nearly linear elastic under small strain and follow a constitutive law based on Hooke's law. Specifically, a ***Hookean elastic solid*** is a solid that obeys Hooke's Law

$$\sigma_{ij} = c_{ijkl}\varepsilon_{kl}, \tag{3.2}$$

where c_{ijkl} is elasticity tensor. If a material is *isotropic*, i.e., the tensor c_{ijkl} is isotropic, then by (3.1) and (3.2) we have

$$\sigma_{ij} = \nu\delta_{ij}\varepsilon_{kk} + 2\mu\varepsilon_{ij}, \tag{3.3}$$

where ν and μ are called *Lamé's parameters*. In engineering literature, the second Lamé parameter is further identified as the *shear modulus*.

3.1.2 Nonlinear elasticity

There exist many cases in which the material remains elastic everywhere but the stress-strain relationship is nonlinear. Examples are a beam under simultaneous lateral and end loads, as well as large deflections of a thin plate or a thin shell. Here we will concentrate on the *hyperelastic* (or *Green elastic*) material, which is an ideally elastic material for which the strain energy density function (a measure of the energy stored in the material as a result of deformation) exists. The behavior of unfilled, vulcanized elastomers often conforms closely to the hyperelastic ideal.

Nonlinear stress-strain relations

Let W denote the strain energy function, which is a scalar function of configuration gradient A defined by (2.5). Then the first Piola-Kirchhoff stress tensor $\mathbf{P}$ is given by

$$\mathbf{P} = \frac{\partial W}{\partial A}, \quad \text{or} \quad P_{ij} = \frac{\partial W}{\partial A_{ij}}, \tag{3.4}$$

where P_{ij} and A_{ij} are the (i,j) components of $\mathbf{P}$ and A, respectively. By (2.6) we can rewrite (3.4) in terms of the Lagrangian strain tensor $\mathbf{E}$,

$$\mathbf{P} = A\frac{\partial W}{\partial \mathbf{E}}, \quad \text{or} \quad P_{ij} = A_{ik}\frac{\partial W}{\partial E_{kj}}. \tag{3.5}$$

By (2.13) and (3.5) we find that the second Piola-Kirchhoff stress tensor $\mathbf{S}$ is given by

$$\mathbf{S} = \frac{\partial W}{\partial \mathbf{E}}, \quad \text{or} \quad S_{ij} = \frac{\partial W}{\partial E_{ij}}, \tag{3.6}$$

where S_{ij} is the (i,j) component of $\mathbf{S}$. By (2.12) and (3.6) we find that the Cauchy stress tensor σ is given by

$$\sigma = \frac{1}{|A|} A \frac{\partial W}{\partial \mathbf{E}} A^T.$$

Strain energy function for isotropic elastic materials

For an isotropic material, the configuration gradient A can be expressed uniquely in terms of the principal stretches $(\lambda_i,\ i = 1,2,3)$ or in terms of the invariants (I_1, I_2, I_3) of the left Cauchy-Green configuration tensor or right Cauchy-Green configuration tensor (see Remark 2.3). Hence, we can express the strain energy function in terms of principal stretches or in terms of invariants. Note that

$$\lambda_1 = \lambda_2 = \lambda_3 = 1, \quad I_1 = 3, \quad I_2 = 3, \quad \text{and} \quad I_3 = 1,$$

in the initial configuration where we choose $W = 0$. Thus a general formula for the strain energy function can be expressed as

$$\begin{aligned} &W(\lambda_1,\lambda_2,\lambda_3) \\ &= \sum_{i,j,k=0}^{\infty} a_{ijk}\Big\{\Big[\lambda_1^i(\lambda_2^j+\lambda_3^j)+\lambda_2^i(\lambda_3^j+\lambda_1^j)+\lambda_3^i(\lambda_1^j+\lambda_2^j)\Big](\lambda_1\lambda_2\lambda_3)^k - 6\Big\}, \end{aligned} \tag{3.7a}$$

or

$$W(I_1,I_2,I_3) = \sum_{i,j,k=0}^{\infty} c_{ijk}(I_1-3)^i(I_2-3)^j(I_3-1)^k. \tag{3.7b}$$

Due to their ubiquitous approximation properties, polynomial terms are usually chosen in formulating strain energy functions, but the final forms are typically based on empirical observations and are material specific for the choice of coefficients and truncations. For incompressible materials (many rubber or elastomeric materials are often nearly incompressible), $|A| = 1$ (which implies that $\lambda_1\lambda_2\lambda_3 = 1$ and $I_3 = 1$), so (3.7a) can be reduced to

$$W(\lambda_1,\lambda_2,\lambda_3) = \sum_{i,j=0}^{\infty} a_{ij}\Big[\lambda_1^i(\lambda_2^j+\lambda_3^j)+\lambda_2^i(\lambda_3^j+\lambda_1^j)+\lambda_3^i(\lambda_1^j+\lambda_2^j)-6\Big], \tag{3.8}$$

subject to

$$\lambda_1\lambda_2\lambda_3 = 1,$$

and (3.7b) can be reduced to

$$W(I_1,I_2) = \sum_{i,j=0}^{\infty} c_{i,j}(I_1-3)^i(I_2-3)^j. \tag{3.9}$$

Special cases for (3.9) include several materials:

1. A Neo-Hookean material for which $W(I_1, I_2) = c_{10}(I_1 - 3)$,
2. A Mooney-Rivilin (or Mooney) material for which

$$W(I_1, I_2) = c_{10}(I_1 - 3) + c_{01}(I_2 - 3).$$

The Neo-Hookean and Mooney-Rivilin strain energy functions have played an important part in the development of nonlinear elasticity theory and its application. The interested reader should consult [24, 44, 48, 59] and the references therein for further information on hyperelastic materials.

3.2 Viscoelastic materials

The distinction between nonlinear elastic and viscoelastic materials is not always easily discerned and definitions vary. However it is generally agreed that viscoelasticity is the property of materials that exhibit both viscous (dashpot-like) and elastic (spring-like) characteristics when undergoing deformation. Food, synthetic polymers, wood, soil and biological soft tissue as well as metals at high temperature display significant viscoelastic effects. Throughout this section, we discuss the concept in a one-dimensional formulation, such as that which occurs in the case of elongation of a simple uniform rod. In more general deformations one must use tensor analogues (as embodied in (3.2)) of the stress, the strain and parameters such as modulus of elasticity and damping coefficient.

In this section we first (Section 3.2.1) introduce some important properties of viscoelastic materials and then discuss the standard dynamic mechanical test in Section 3.2.2. We then present and discuss a number of specific forms of constitutive equations proposed in the literature for linear viscoelastic materials (Section 3.2.3) and those for nonlinear viscoelastic materials (Section 3.2.4).

3.2.1 Properties of viscoelastic materials

Viscoelastic materials are those for which the relationship between stress and strain depends on time, and they possess the following three important properties: *stress relaxation* (a step constant strain results in decreasing stress), *creep* (a step constant stress results in increasing strain), and *hysteresis* (a stress-strain phase lag).

Stress relaxation

In a stress relaxation test, a constant strain ε_0 acts as "input" to the material from time t_0, the resulting time-dependent stress is decreasing until a plateau is reached at some later time, which is as depicted in Fig. 4. The stress function $G(t)$ resulting from the unit step strain (that is, $\varepsilon_0 = 1$) is referred to as the *relaxation modulus*.

In a stress relaxation test, viscoelastic solids gradually relax and reach an equilibrium stress greater than zero, i.e.,

$$\lim_{t\to\infty} G(t) = G_\infty > 0,$$

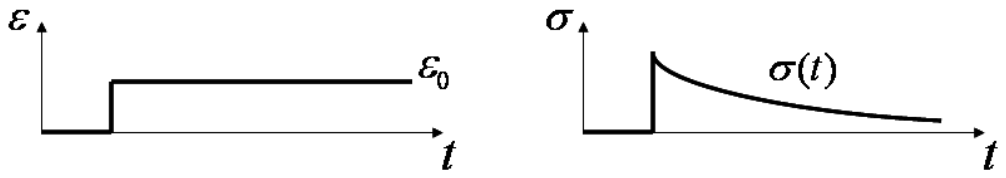

Figure 4: Stress and strain histories in the stress relaxation test.

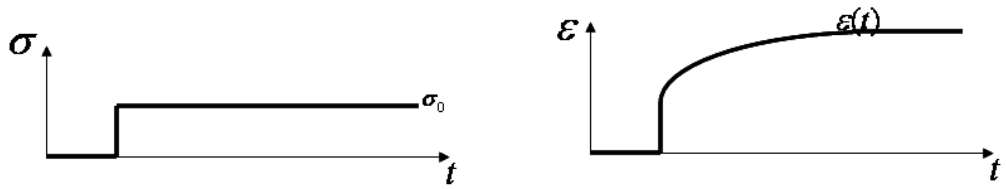

Figure 5: Stress and strain histories in the creep test.

while for viscoelastic fluids the stress vanishes to zero, i.e.,

$$\lim_{t\to\infty} G(t) = 0.$$

Creep

In a creep test, a constant stress σ_0 acts as "input" to the material from time t_0, the resulting time-dependent strain is increasing as depicted in Fig. 5.

The strain function $J(t)$ resulting from the unit step stress (i.e., $\sigma_0 = 1$) is called the *creep compliance*.

In a creep test, the resulting strain for viscoelastic solids increases until it reaches a nonzero equilibrium value, i.e.,

$$\lim_{t\to\infty} J(t) = J_\infty > 0,$$

while for viscoelastic fluids the resulting strain increases without bound as t increases.

Hysteresis

Hysteresis can be seen from the stress-strain curve which reveals that for a viscoelastic material the loading process is different than in the unloading process. For example, the left plot in Fig. 6 illustrates the associated stress-strain curve for the Hookean elastic solid, and that in the right plot of Fig. 6 is for the Kelvin-Voigt model (a linear viscoelastic model discussed below in Section 3.2.3). From this figure, we see that we can differentiate between the loading and unloading for the Kelvin-Voigt material, but we cannot do this for Hookean elastic material. Thus the Kelvin-Voigt material "remembers" whether it is being loaded or unloaded, hence exhibiting "hysteresis" in the material.

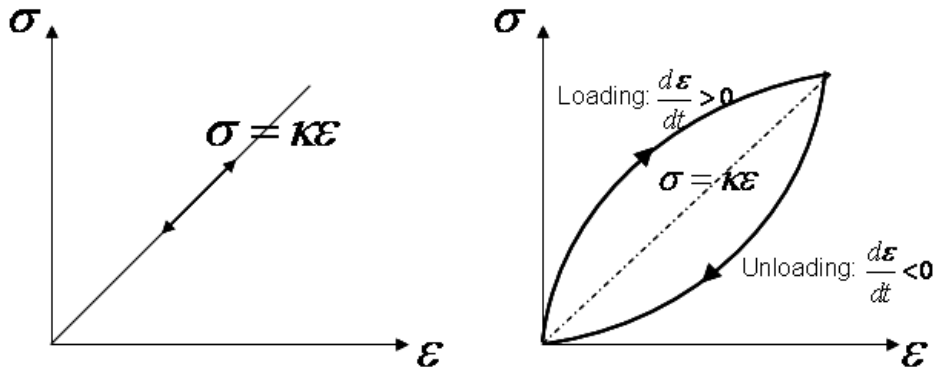

(a) (b)

Figure 6: Stress and strain curves during cyclic loading-unloading. (a): Hookean elastic solid; (b) Kelvin-Voigt material depicted by the solid line.

3.2.2 Dynamic mechanical tests: stress-strain phase lag, energy loss and complex dynamic modulus

In addition to the creep and stress relaxation tests, a dynamic test is useful in studying the behavior of viscoelastic materials. Stress (or strain) resulting from a small strain (or stress) is measured and can be used to find the complex dynamic modulus as introduced below. We illustrate these ideas with a discussion of the stress resulting from a sinusoidal strain (as the discussion in the strain resulting from an analogous stress can proceed similarly by just interchanging the role of stress and strain).

In a typical dynamic test carried out at a constant temperature, one programs a loading machine to prescribe a cyclic history of strain to a sample rod given by

$$\varepsilon(t) = \varepsilon_0 \sin(\omega t), \tag{3.10}$$

where ε_0 is the amplitude (assumed to be small), and ω is the angular frequency. The response of stress as a function of time t depends on the characteristics of the material which can be separated into several categories:

• A purely elastic solid.

For this material, stress is proportional to the strain, i.e., $\sigma(t) = \kappa\varepsilon(t)$. Hence with the strain defined in (3.10), the stress is given by

$$\sigma(t) = \kappa\varepsilon_0 \sin(\omega t).$$

We find the stress amplitude σ_0 is linear in the strain amplitude ε_0: $\sigma_0 = \kappa\varepsilon_0$. The response of stress caused by strain is immediate. That is, the stress is *in phase* with the strain.

• A purely viscous material.

For this kind of material, stress is proportional to the strain rate: $\sigma(t) = \eta d\varepsilon/dt$. For the strain defined in (3.10), the stress is then given by

$$\sigma(t) = \eta\epsilon_0\omega \cos(\omega t).$$

Note that

$$\cos(\omega t) = \sin\left(\omega t + \frac{\pi}{2}\right),$$

and thus we can rewrite the above expression as

$$\sigma(t) = \eta\epsilon_0\omega \sin\left(\omega t + \frac{\pi}{2}\right).$$

The stress amplitude is linear in the strain amplitude: $\sigma_0 = \eta\epsilon_0\omega$, which is dependent on the frequency ω. The stress is out of phase with the strain, and strain lags stress by a 90 degree phase lag.

• A linear viscoelastic solid.

With the sinusoidal strain (3.10), the stress as a function of time appears complicated in the first few cycles. But a steady state will eventually be reached in which the resulting stress is also sinusoidal, having the same angular frequency ω but retarded in phase by an angle δ. This is true even if the stress rather than the strain is the controlled variable. The cyclic stress is written as

$$\sigma(t) = \sigma_0 \sin(\omega t + \delta), \tag{3.11}$$

where the phase shift δ is between 0 and $\pi/2$, and the stress amplitude σ_0 depends on the frequency ω. By an identity of trigonometry, we can rewrite (3.11) as

$$\sigma(t) = \sigma_0 \cos(\delta) \sin(\omega t) + \sigma_0 \sin(\delta) \cos(\omega t). \tag{3.12}$$

Thus the stress is the sum of an in-phase response and out-of-phase response.

We consider the energy loss for a linear viscoelastic material such as described by the stress (3.11) in response to the strain input (3.10). Let l be the length of a rod with cross sectional area a. When the solid is strained sinusoidally, according to (3.10), the solid elongates as

$$\Delta l(t) = l\varepsilon_0 \sin(\omega t).$$

By (3.12), the force on the rod is

$$F(t) = a\sigma(t) = a\sigma_0 \cos(\delta) \sin(\omega t) + a\sigma_0 \sin(\delta) \cos(\omega t).$$

During a time interval dt, the solid elongates by $d\Delta l$, and the work done on the rod is

$$F(t)d\Delta l = F(t)\frac{d\Delta l}{dt}dt = l\varepsilon_0\omega F(t) \cos(\omega t)dt.$$

In one full cycle the work done is

$$\begin{aligned} W =& al\varepsilon_0\sigma_0\omega \cos(\delta) \int_0^{\frac{2\pi}{\omega}} \sin(\omega t) \cos(\omega t)dt + al\varepsilon_0\sigma_0\omega \sin(\delta) \int_0^{\frac{2\pi}{\omega}} \cos(\omega t) \cos(\omega t)dt \\ =& \pi al\varepsilon_0\sigma_0 \sin(\delta). \end{aligned}$$

Note that the in-phase components produce no net work when integrated over a cycle, while the out-of phase components result in a net dissipation per cycle equal to:

$$W = \pi a l \varepsilon_0 \sigma_0 \sin(\delta).$$

Thus, for a purely elastic solid, the stress is in phase with the strain ($\delta = 0$) and no energy is dissipated. On the other hand, motion in the viscoelastic solid produces energy loss.

It is a common practice in engineering to use complex variables to describe the sinusoidal response of viscoelastic materials. Thus, instead of strain history (3.10), we specify the complex strain as

$$\varepsilon^* = \varepsilon_0 \exp(i\omega t).$$

Then we obtain the following complex stress instead of stress described by (3.11)

$$\sigma^* = \sigma_0 \exp\big(i(\omega t + \delta)\big).$$

The above equation can be rewritten as

$$\sigma^* = G^* \varepsilon^*,$$

where G^* is defined by

$$G^* = \frac{\sigma_0}{\varepsilon_0} \exp(i\delta) = \frac{\sigma_0}{\varepsilon_0} \cos(\delta) + i \frac{\sigma_0}{\varepsilon_0} \sin(\delta). \tag{3.13}$$

The characteristic parameter G^* is referred to as the *complex dynamic modulus*. We denote the real part of G^* by G' and the imaginary part of G^* by G''. That is,

$$G^* = G' + iG'', \tag{3.14}$$

where

$$G' = \frac{\sigma_0}{\varepsilon_0} \cos(\delta), \quad \text{and} \quad G'' = \frac{\sigma_0}{\varepsilon_0} \sin(\delta).$$

The coefficient G' is called the *storage modulus* (a measure of energy stored and recovered per cycle) which corresponds to the in-phase response, and G'' is the *loss modulus* (a characterization of the energy dissipated in the material by internal damping) corresponding to the out-of phase response. The in-phase stress and strain results in elastic energy, which is completely recoverable. The $\pi/2$ out-of-phase stress and strain results in the dissipated energy.

Remark 3.3. The relationship between the two transient functions, relaxation modulus $G(t)$ and creep compliance $J(t)$, for a viscoelastic material is given by

$$\int_0^t J(s)G(t-s)ds = t.$$

The relationship between the relaxation modulus $G(t)$ and dynamic modulus functions G' and G'' is given by

$$G'(\omega) = G_\infty + \omega \int_0^\infty \big(G(t) - G_\infty\big) \sin(\omega t) dt,$$
$$G''(\omega) = \omega \int_0^\infty \big(G(t) - G_\infty\big) \cos(\omega t) dt.$$

The relations may be inverted to obtain

$$G(t) = G_\infty + \frac{2}{\pi} \int_0^\infty \frac{G'(\omega) - G_\infty}{\omega} \sin(\omega t) d\omega,$$

or

$$G(t) = G_\infty + \frac{2}{\pi} \int_0^\infty \frac{G''(\omega)}{\omega} \cos(\omega t) d\omega.$$

The interested reader can refer to the recent text [33] for further information.

3.2.3 Linear viscoelastic models: constitutive relationships

The characteristic feature of linear viscoelastic materials is that the stress is linearly proportional to the strain history, and it is important to note that the property of linearity of response does not refer to the shape of any material response curve. Linear viscoelasticity is usually applicable only for small deformations and/or linear materials. Thus, infinitesimal strain theory should be employed for this case. There are two standard approaches that have been used to develop constitutive equations for the linear viscoelastic materials: mechanical analogs and the Boltzmann superposition principle.

Mechanical analogs

Linear viscoelastic behavior can be conceived as a linear combinations of springs (the elastic component) and dashpots (the viscous component) as depicted by Fig. 7. The elastic component is described by

$$\sigma = \kappa \varepsilon,$$

or

$$\frac{d\varepsilon}{dt} = \frac{1}{\kappa} \frac{d\sigma}{dt},$$

where σ is the stress, ε is the strain that occurs under the given stress, and κ is the elastic modulus of the material with units $\mathrm{N/m^2}$. The viscous component is modeled by

$$\sigma = \eta \frac{d\varepsilon}{dt},$$

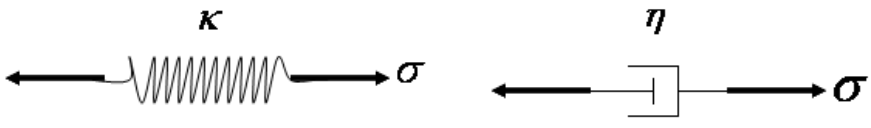

(a) (b)

Figure 7: (a): Schematic representation of the Hookean spring; (b) Schematic representation of Newtonian dashpot.

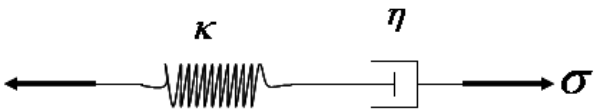

Figure 8: Schematic representation of the Maxwell model.

where η is the viscosity of the material with units $\mathrm{N}\cdot\mathrm{s}/\mathrm{m}^2$. The mechanical analogues approach results in a linear ordinary differential equation with constant coefficients relating stress and its rates of finite order with strain and its rates of the form

$$a_0\sigma + a_1\frac{d\sigma}{dt} + a_2\frac{d^2\sigma}{dt^2} + \cdots + a_n\frac{d^n\sigma}{dt^n} = b_0\varepsilon + b_1\frac{d\varepsilon}{dt} + b_2\frac{d^2\varepsilon}{dt^2} + \cdots + b_n\frac{d^n\varepsilon}{dt^n}. \tag{3.15}$$

In (3.15) the constant coefficients a_i, b_i, $i = 0, 1, 2, \cdots, n$ are related to the elastic modulus and viscosity of the material which are usually determined from physical experiments. A complete statement of the constitutive equation obtained from use of mechanical analogs then consists of both an equation of the form (3.15) and a set of appropriate initial conditions. In addition, we see that it is not convenient to directly incorporate this general model (3.15) into the equation of motion.

The three basic models that are typically used to model linear viscoelastic materials are the Maxwell model, the Kelvin-Voigt model and the standard linear solid model. Each of these models differs in the arrangement of these "springs" and "dashpots".

The Maxwell model

The Maxwell model is represented by a purely viscous damper and a purely elastic spring connected in series as depicted in Fig. 8.

Because the spring and the dashpot are subject to the same stress, the model is also known as an iso-stress model. The total strain rate is the sum of the elastic and the viscous strain contributions, so that

$$\frac{\sigma}{\eta} + \frac{1}{\kappa}\frac{d\sigma}{dt} = \frac{d\varepsilon}{dt}. \tag{3.16}$$

We consider the stress relaxation function and creep function for the Maxwell model (3.16). The stress relaxation function corresponds to the relaxation that occurs under an imposed constant strain, given

$$\varepsilon(t) = \varepsilon_0 H(t - t_0), \quad \text{and} \quad \sigma(0) = 0,$$

where $H(t)$ is the *Heaviside step function* (also called the *unit step function* in the literature), $t_0 \geq 0$. The solution $\sigma(t)$ to (3.16) is the *relaxation function*. With this strain function, (3.16) can be written as

$$\frac{\sigma}{\eta} + \frac{1}{\kappa}\frac{d\sigma}{dt} = \varepsilon_0 \delta(t - t_0),$$

where δ is the Dirac delta function. Let

$$\hat{\sigma}(s) = \mathscr{L}\{\sigma(t)\}(s),$$

where $\mathscr{L}$ denotes the Laplace transform. Then taking the Laplace transform of both sides of the above differential equation we obtain

$$\hat{\sigma}(s) = \varepsilon_0 e^{-t_0 s}\Big(\frac{1}{\eta} + \frac{1}{\kappa}s\Big)^{-1} = \kappa\varepsilon_0 e^{-t_0 s}\Big(s + \frac{\kappa}{\eta}\Big)^{-1}.$$

Taking the inverse Laplace transform one finds that

$$\sigma(t) = \kappa \exp\Big[-\frac{\kappa}{\eta}(t - t_0)\Big]\varepsilon_0 H(t - t_0).$$

The stress relaxation function for the Maxwell model (3.16) is illustrated in Fig. 9 (compare with Fig. 4).

The creep function corresponds to the creep that occurs under the imposition of a constant stress given by

$$\sigma(t) = \sigma_0 H(t - t_0), \quad \text{and} \quad \varepsilon(0) = 0,$$

the solution $\varepsilon(t)$ to (3.16) is the *creep function*. With this stress function, (3.16) can be written as

$$\frac{d\varepsilon}{dt} = \frac{\sigma_0}{\eta}H(t - t_0) + \frac{\sigma_0}{\kappa}\delta(t - t_0).$$

Then taking the Laplace transform of both sides of the above differential equation we have that

$$\hat{\varepsilon}(s) = \frac{\sigma_0}{\eta}\frac{e^{-t_0 s}}{s^2} + \frac{\sigma_0}{\kappa}\frac{e^{-t_0 s}}{s}.$$

Upon taking the inverse Laplace transform we find

$$\varepsilon(t) = \Big[\frac{1}{\kappa} + \frac{1}{\eta}(t - t_0)\Big]\sigma_0 H(t - t_0).$$

The creep function of Maxwell model (3.16) is illustrated in Fig. 10 (again, compare with Fig. 5).

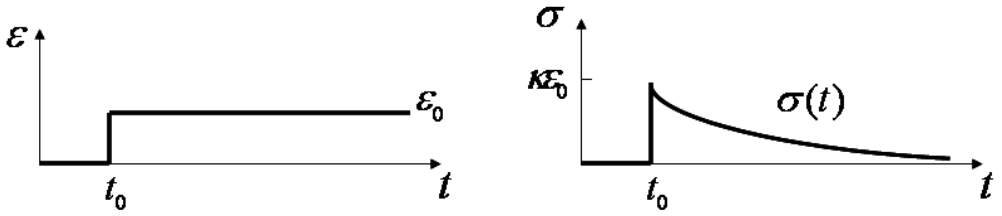

Figure 9: Stress relaxation function of Maxwell model.

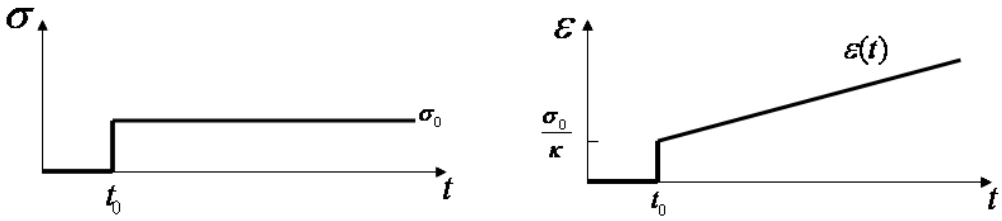

Figure 10: Creep function of Maxwell model.

From the above considerations we see that the Maxwell model predicts that stress decays exponentially with time, which is accurate for many materials, especially polymers. However, a serious limitation of this model (with creep as depicted in Fig. 10) is its inability to correctly represent the creep response of solid material which does not increase without bound. Indeed polymers frequently exhibit decreasing strain rate with increasing time.

Finally we find the storage modulus G' and loss modulus G'' for the Maxwell model. Let

$$\varepsilon(t) = \varepsilon_0 \exp(i\omega t), \quad \text{and} \quad \sigma(t) = \sigma_0 \exp\big(i(\omega t + \delta)\big).$$

Then we substitute ε and σ into (3.16) which after some algebraic arguments results in the complex dynamic modulus

$$G^* = \frac{\sigma_0}{\varepsilon_0} \exp(i\delta) = \frac{\kappa(\eta\omega)^2}{\kappa^2 + (\eta\omega)^2} + i\frac{\kappa^2\eta\omega}{\kappa^2 + (\eta\omega)^2}.$$

For the storage and loss modulus we thus find

$$G' = \frac{\kappa(\eta\omega)^2}{\kappa^2 + (\eta\omega)^2}, \qquad G'' = \frac{\kappa^2\eta\omega}{\kappa^2 + (\eta\omega)^2}.$$

By taking the derivative of G'' with respect to frequency ω, we find that the loss modulus achieves its maximum value at $\omega = 1/\tau$, where $\tau = \eta/\kappa$ is the relaxation time.

The Kelvin-Voigt model

The Kelvin-Voigt model, also known as the Voigt model, consists of a Newtonian damper and a Hookean elastic spring connected in parallel, as depicted in Fig. 11.

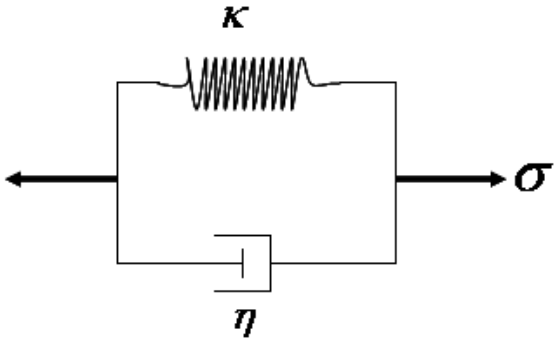

Figure 11: Schematic representation of the Kelvin-Voigt model.

Because the two elements are subject to the same strain, the model is also known as an iso-strain model. The total stress is the sum of the stress in the spring and the stress in the dashpot, so that

$$\sigma = \kappa\varepsilon + \eta\frac{d\varepsilon}{dt}. \tag{3.17}$$

We first consider the stress relaxation function and creep function for the Kelvin-Voigt model (3.17). The stress relaxation function corresponds to the solution of (3.17) when

$$\varepsilon(t) = \varepsilon_0 H(t - t_0), \quad \text{and} \quad \sigma(0) = 0.$$

We find

$$\sigma(t) = \kappa\varepsilon_0 H(t - t_0) + \eta\varepsilon_0\delta(t - t_0).$$

This stress relaxation function for the Kelvin-Voigt model (3.17) is illustrated in Fig. 12.

The creep function again is the solution $\varepsilon(t)$ to (3.17) corresponding to $\sigma(t) = \sigma_0 H(t - t_0)$ and $\varepsilon(0) = 0$. We find

$$\kappa\varepsilon + \eta\frac{d\varepsilon}{dt} = \sigma_0 H(t - t_0).$$

Let $\hat{\varepsilon}(s) = \mathscr{L}\{\varepsilon(t)\}(s)$, or in terms of the Laplace transform we have

$$\hat{\varepsilon}(s) = \sigma_0\frac{e^{-t_0 s}}{s(\kappa + \eta s)} = \frac{\sigma_0}{\kappa}\Big[\frac{e^{-t_0 s}}{s} - \frac{e^{-t_0 s}}{s + \kappa/\eta}\Big].$$

Using the inverse Laplace transform we obtain

$$\varepsilon(t) = \frac{1}{\kappa}\Big[1 - \exp\Big(-\frac{\kappa}{\eta}(t - t_0)\Big)\Big]\sigma_0 H(t - t_0).$$

The corresponding creep function for the Kelvin-Voigt model (3.17) is illustrated in Fig. 13 (compare with Fig. 5).

Thus we find that the Kelvin-Voigt model is extremely accurate in modelling creep in many materials. However, the model has limitations in its ability to describe the commonly observed relaxation of stress in numerous strained viscoelastic materials.

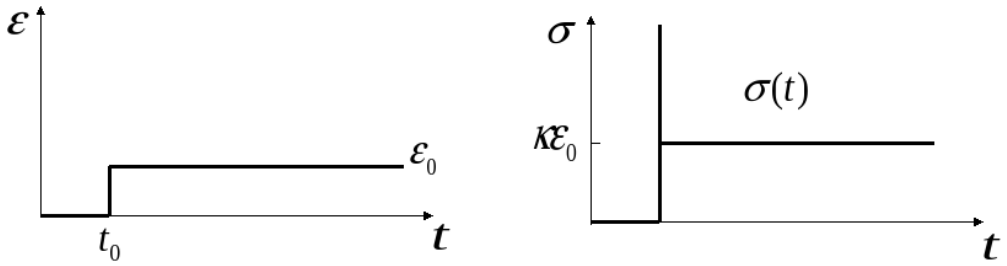

Figure 12: Stress relaxation function for the Kelvin-Voigt model.

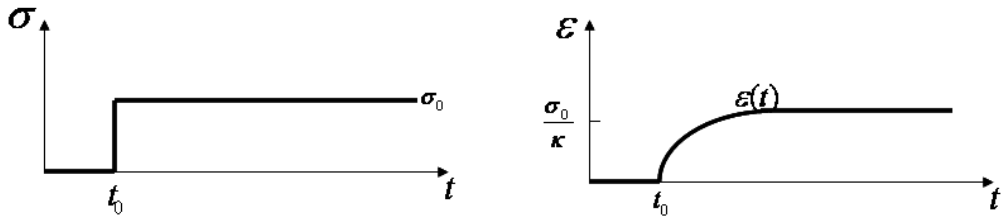

Figure 13: Creep function of Kelvin-Voigt model.

Finally we may obtain the storage modulus G' and loss modulus G'' for the Kelvin-Voigt model (3.17). Letting

$$\varepsilon(t) = \varepsilon_0 \exp(i\omega t), \quad \text{and} \quad \sigma(t) = \sigma_0 \exp\big(i(\omega t + \delta)\big),$$

and substituting ε and σ into (3.17), we find

$$G^* = \frac{\sigma_0}{\varepsilon_0} \exp(i\delta) = \kappa + i\eta\omega.$$

Hence, by (3.14) we have

$$G' = \kappa, \qquad G'' = \eta\omega.$$

Remark 3.4. Because of one of our motivating applications (discussed in Section 4 below), we are particularly interested in the elastic/viscoelastic properties of soil. Hardin in [31] presented an analytical study of the application of the Kelvin-Voigt model to represent dry soils for comparison with test results. From this study he found that the Kelvin-Voigt model satisfactorily represented the behavior of sands in these small-amplitude vibration tests if the viscosity η in the model was treated as varying inversely with the frequency ω to maintain the ratio $\eta\omega/\kappa$ constant. Since Hardin's work, describing soils as a Kelvin-Voigt material has become accepted as one of the best ways in soil dynamics of calculating wave propagation and energy dissipation. The Kelvin-Voigt model also governs the analysis of standard soil tests, including consolidation and resonant-column tests. The interested reader can refer to [40, 41, 47] as well as the references therein for more information of the model's historical backgrounds and examples of its application in soil dynamics.

It is interesting to note that the author in [13] showed that the Kelvin-Voigt model can be used to describe the dynamic response of the saturated poroelastic materials

that obey the Biot theory (the two-phase formulation of Biot in [15]). This viscoelastic model is simpler to use than poroelastic models but yields similar results for a wide range of soils and dynamic loadings. In addition, the author in [40] developed a model, the Kelvin-Voigt-Maxwell-Biot model, that splits the soil into two components (pore fluid and solid frame) where these two masses are connected by a dashpot which can then be related to permeability. In addition, a mapping between the Kelvin-Voigt model and the Kelvin-Voigt-Maxwell-Biot model is developed in [40] so that one may continue to use the Kelvin-Voigt model for saturated soil.

The standard linear solid (SLS) model

The standard linear solid model, also known as the Kelvin model or *three-element model*, combines the Maxwell Model and a Hookean spring in parallel as depicted in Fig. 14.

The stress-strain relationship is given by

$$\sigma + \tau_\varepsilon \frac{d\sigma}{dt} = \kappa_r \left(\varepsilon + \tau_\sigma \frac{d\varepsilon}{dt} \right), \tag{3.18}$$

where

$$\tau_\varepsilon = \frac{\eta_1}{\kappa_1}, \quad \text{and} \quad \tau_\sigma = \eta_1 \frac{\kappa_r + \kappa_1}{\kappa_r \kappa_1},$$

from which can be observed that $\tau_\sigma > \tau_\varepsilon$.

The stress relaxation function and the creep function for the standard linear model (3.18) are obtained in the usual manner. As usual, the stress relaxation function $\sigma(t)$ is obtained by solving (3.18) with $\varepsilon(t) = \varepsilon_0 H(t - t_0)$ and $\sigma(0) = 0$. We find

$$\sigma(t) + \tau_\varepsilon \frac{d\sigma}{dt} = \kappa_r \varepsilon_0 H(t - t_0) + \kappa_r \tau_\sigma \varepsilon_0 \delta(t - t_0),$$

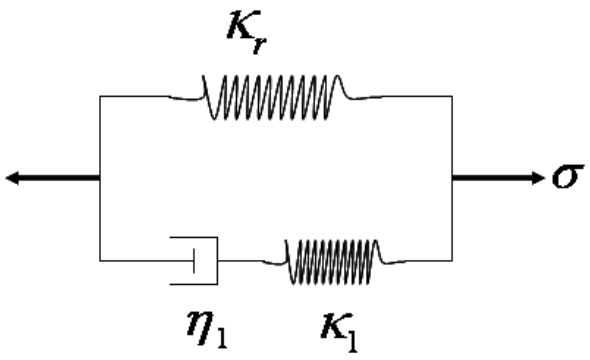

Figure 14: Schematic representation of the standard linear model.

or in terms of the Laplace transform

$$\begin{aligned}\hat{\sigma}(s) =&\kappa_r\varepsilon_0\frac{e^{-t_0 s}}{s(1+\tau_\varepsilon s)}+\kappa_r\tau_\sigma\varepsilon_0\frac{e^{-t_0 s}}{1+\tau_\varepsilon s}\\ =&\kappa_r\varepsilon_0\frac{e^{-t_0 s}}{s}+\kappa_r\varepsilon_0\Big(\frac{\tau_\sigma}{\tau_\varepsilon}-1\Big)\frac{e^{-t_0 s}}{s+\frac{1}{\tau_\varepsilon}}.\end{aligned}$$

Thus we find

$$\begin{aligned}\sigma(t) =&\kappa_r\varepsilon_0 H(t-t_0)+\kappa_r\varepsilon_0\Big(\frac{\tau_\sigma}{\tau_\varepsilon}-1\Big)\exp\Big[-\frac{t-t_0}{\tau_\varepsilon}\Big]H(t-t_0)\\ =&\kappa_r\Big[1+\Big(\frac{\tau_\sigma}{\tau_\varepsilon}-1\Big)\exp\Big(-\frac{t-t_0}{\tau_\varepsilon}\Big)\Big]\varepsilon_0 H(t-t_0)\\ =&\Big[\kappa_r+\kappa_1\exp\Big(-\frac{t-t_0}{\tau_\varepsilon}\Big)\Big]\varepsilon_0 H(t-t_0).\end{aligned}$$

This stress relaxation function for the standard linear model (3.18) is illustrated in Fig. 15.

The creep function is the solution of (3.18) for $\varepsilon(t)$ given $\sigma(t)=\sigma_0 H(t-t_0)$ and $\varepsilon(0)=0$. Using the same arguments as above in finding the stress function, we have

$$\varepsilon(t)=\frac{1}{\kappa_r}\Big[1+\Big(\frac{\tau_\varepsilon}{\tau_\sigma}-1\Big)\exp\Big(-\frac{t-t_0}{\tau_\sigma}\Big)\Big]\sigma_0 H(t-t_0).$$

The creep function of the standard linear model (3.18) is illustrated in Fig. 16.

We therefore see that the standard linear model is accurate in predicating both creep and relaxation responses for many materials of interest.

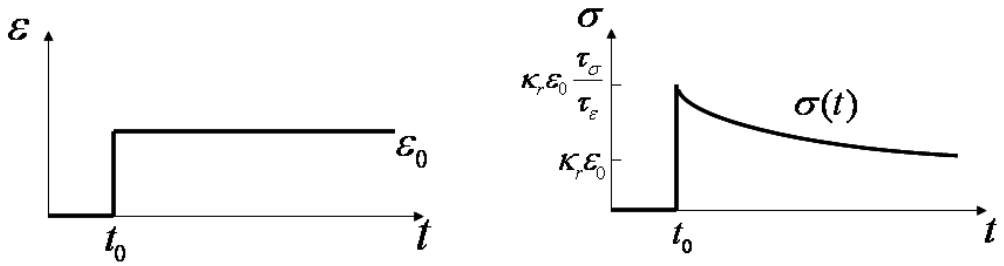

Figure 15: Stress relaxation function for the standard linear model.

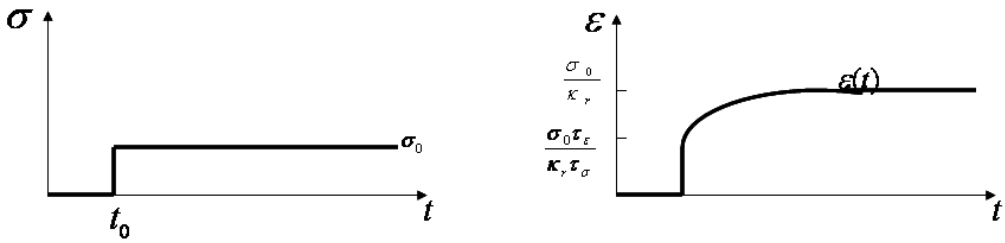

Figure 16: Creep function for the standard linear model.

Finally the usual arguments for the standard linear model lead to

$$G^* = \frac{\sigma_0}{\varepsilon_0}\exp(i\delta) = \frac{\kappa_r(1+\tau_\sigma\tau_\varepsilon\omega^2)}{1+(\tau_\epsilon\omega)^2} + i\frac{\kappa_r(\tau_\sigma-\tau_\varepsilon)\omega}{1+(\tau_\epsilon\omega)^2}.$$

By definition of the storage and loss modulus, we thus have

$$G' = \frac{\kappa_r(1+\tau_\sigma\tau_\varepsilon\omega^2)}{1+(\tau_\epsilon\omega)^2}, \qquad G'' = \frac{\kappa_r(\tau_\sigma-\tau_\varepsilon)\omega}{1+(\tau_\epsilon\omega)^2}.$$

Remark 3.5. It was demonstrated in [45] that the relaxation behavior of compressed wood can be adequately described by the standard-linear-model.

The Boltzmann superposition model

A general approach widely used to model linear viscoelastic materials is due to Boltzmann (1844-1906) and is called the Boltzmann superposition model or simply the Boltzmann model.

If the origin for time is taken at the beginning of motion and loading (i.e., $\sigma(0) = 0$ and $\varepsilon(0) = 0$), then the stress-strain law is given by

$$\sigma(t) = \kappa_r\varepsilon(t) + \int_0^t K(t-s)\frac{d\varepsilon(s)}{ds}ds, \tag{3.19}$$

where κ_r represents an instantaneous relaxation modulus, and K is the "gradual" relaxation modulus function. The relaxation modulus function $G(t)$ for the Boltzmann model (3.19) is given by

$$G(t) = \kappa_r + K(t).$$

Note that $\epsilon(0) = 0$. Hence, (3.19) can be rewritten as follows

$$\sigma(t) = \int_0^t G(t-s)\frac{d\varepsilon(s)}{ds}ds. \tag{3.20}$$

If the strain $\epsilon(t)$ has a step discontinuity at $t = 0$, then by integration of the resulting delta function for its derivative we obtain the following representation from (3.20)

$$\sigma(t) = G(t)\varepsilon(0) + \int_0^t G(t-s)\frac{d\varepsilon(s)}{ds}ds. \tag{3.21}$$

This results in a decaying stress if the strain is held constant after a step discontinuity. The interested reader can refer to [16, pp. 5–6] for more information on the connection of several different forms of the Boltzmann superposition model.

We find that when model (3.19) is incorporated into force balance laws (equation of motion), it results in integro-partial differential equations which are most often phenomenological in nature as well as being computationally challenging both in simulation and control design.

Remark 3.6. Any constitutive equation of form (3.15), along with the appropriate initial conditions, can be expressed in either the form (3.19) (or (3.21)) or its corresponding compliance form (i.e., the strain in terms of the stress and stress rate). On the other hand, a constitutive equation of form (3.19) (or (3.21)) can be reduced to the form (3.15) if and only if the stress relaxation modulus satisfy specific conditions. A detailed discussion of this can be found in [28]. For example, the Maxwell, Kelvin-Voigt, and standard linear models can be expressed in the Boltzmann formulation. The choice of parameters in (3.19) to yield these models are readily verified to be:

1. The Maxwell model: $\kappa_r = 0$, and $K(t-s) = \kappa \exp\big[-(t-s)/\tau\big]$ with $\tau = \eta/\kappa$;
2. The Kelvin-Voigt model: $\kappa_r = \kappa$, and $K(t-s) = \eta\delta(t-s)$;
3. The standard linear model: $K(t-s) = \big(\tau_\sigma/\tau_\varepsilon - 1\big)\kappa_r \exp\big[-(t-s)/\tau_\varepsilon\big]$, which can be simplified as $K(t-s) = \kappa_1 \exp\big[-(t-s)/\tau_\varepsilon\big]$ with $\tau_\varepsilon = \eta_1/\kappa_1$.

Internal variable approach

Other special cases of (3.19) that are often encountered include a generalization of the single spring-dashpot paradigm of Fig. 14 (the standard linear model) to one with multiple spring-dashpot systems in parallel as depicted in Fig. 17. This is a generalized standard linear model (also referred to as *generalized Maxwell model* or *Wiechert model* or *Maxwell-Wiechert model* in the literature) that results in the relaxation response kernel

$$K(t-s) = \sum_{j=1}^{n} \kappa_j \exp\Big(-\frac{t-s}{\tau_j}\Big), \tag{3.22}$$

where $\tau_j = \eta_j/\kappa_j$, $j = 1, 2, \cdots, n$. We observe that the Boltzmann formulation with relaxation response kernel (3.22) is equivalent to the formulation

$$\sigma(t) = \kappa_r \varepsilon(t) + \sum_{j=1}^{n} \kappa_j \varepsilon_j(t), \tag{3.23}$$

where the ε_j satisfy the following ordinary differential equations

$$\frac{d\varepsilon_j(t)}{dt} + \frac{1}{\tau_j}\varepsilon_j(t) = \frac{d\varepsilon(t)}{dt}, \quad \varepsilon_j(0) = 0, \quad j = 1, 2, \cdots, n. \tag{3.24}$$

The formulation (3.23) with (3.24) is sometimes referred to as an *internal variable* model (e.g., see [7,12]–for other discussions of internal state variable approaches, see also [35, 36, 51–53]) because the variables ε_j can be thought of as "internal strains" that are driven by the instantaneous strain according to (3.24) and that contribute to the total stress via (3.23). Hence, we can see that this internal variable modeling leads to an efficient computational alternative for the corresponding integro-partial differential equation models involving (3.19). In addition, we note that this approach provides a "molecular" basis for the models as it can be thought of as a model for a heterogeneous material containing multiple types of molecules [7,12,19,32], each possessing a

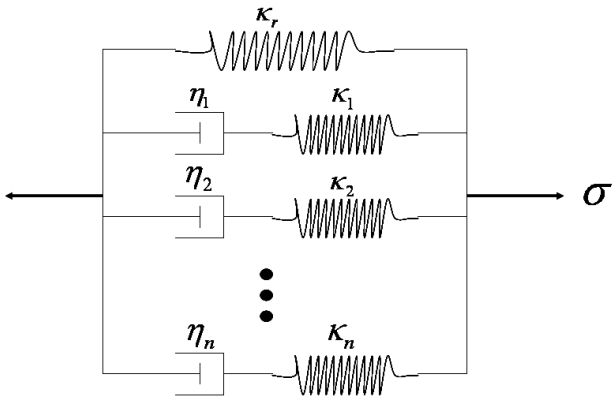

Figure 17: Schematic representation of the generalized standard linear model.

distinct relaxation property characterized by a relaxation parameter τ_j. For a comparison of models of viscoelastic damping via hysteretic integrals versus internal variable representations, see [7] and the references therein.

Moreover, we see that model (3.23) with (3.24) can be readily viewed as a special case of or even an approximation to models with a continuum of relaxation times (see [12] and the references therein). These models have proved useful in a wide range of viscoelastic materials. The corresponding stress-strain laws have the form

$$\sigma(t;\mathcal{P}) = \kappa_r \varepsilon(t) + \eta \frac{d\varepsilon(t)}{dt} + \gamma \int_{\mathcal{T}} \varepsilon_1(t;\tau) d\mathcal{P}(\tau), \tag{3.25}$$

where $\mathcal{P}$ is a probability distribution over the set $\mathcal{T}$ of possible relaxation parameters τ, and $\varepsilon_1(t;\tau)$ satisfies, for each $\tau \in \mathcal{T}$,

$$\frac{d\varepsilon_1(t;\tau)}{dt} + \frac{1}{\tau}\varepsilon_1(t;\tau) = \frac{d\varepsilon(t)}{dt}, \qquad \varepsilon_1(0;\tau) = 0. \tag{3.26}$$

The approach embodied in equations (3.25)-(3.26) offers a computationally tractable alternative for linear materials with a continuum of relaxation times.

Remark 3.7. The generalized standard linear model (i.e., model (3.23) combined with (3.24)) with different n has been successfully used to describe the stress relaxation behavior of a variety of foods. For example, in [57] this model with $n = 2$ was successfully used to describe the stress relaxation of lipids such as beeswax, candelilla wax, carnauba wax and a high melting point milkfat fraction. A comprehensive study on the ability of the generalized Maxwell model to describe the stress relaxation behavior of solid food is presented in [18]. In this study, five different food matrices (agar gel, meat, ripened cheese, "mozzarella" cheese and white pan bread) were chosen as representatives of a wide range of foods, and results verify that the proposed model satisfactorily fits the experimental data.

3.2.4 Nonlinear viscoelasticity: constitutive relationships

For many materials the linear models given in Section 3.2.3 are inadequate to describe experimental data. In particular, shape memory alloys such as Nitinol (a nickel-titanium) and CuZnAl (a cooper zinc aluminum aloy), biological soft tissue and highly filled rubber exhibit significant nonlinear hysteric behavior such as that depicted by the experimental data for highly filled rubber given in Fig. 18. Nonlinear viscoelastic behavior is usually exhibited when the deformation is large or if the material changes its properties under deformations.

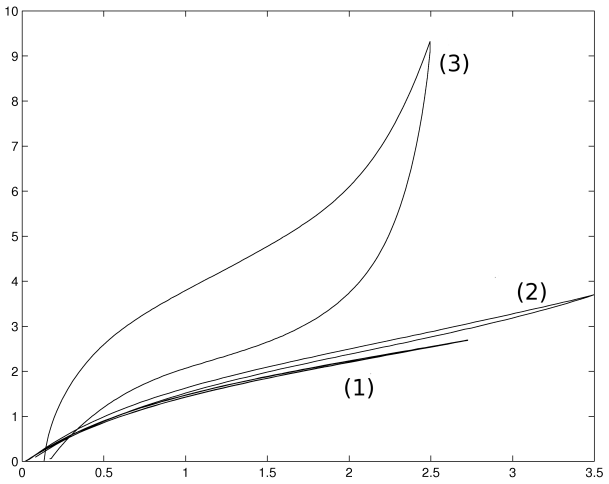

Figure 18: Experimental stress-strain curves for (1) unfilled, (2) lightly filled and (3) highly filled rubber in tensile deformations.

The theory of nonlinear viscoelasticity has attracted the attention of a large number of investigators over the past century (e.g., [19,20,23,25,37,42,53,58]). Two types of models for stress-strain relationships can be found in the literature. One is based on the phenomenological mechanical behavior of the materials (that is, the form of constitutive equations is not based on the explanation of how these properties arise from the underlying microscopic structure). For example, Green and Rivlin in [27] constructed a multiple integral constitutive equation, which is arranged as a series in which the nth term is of degree n in the strain components. A multiple integral constitutive equation, arranged in a series, was also developed by Pipkin and Rogers in [46], in which the first term gives the results of a one-step test (the stress due to a step change of strain), and whose nth term represents a correction due to the nth step. The interested reader can refer to [20,61] for recent historical overviews on these phenomenological models as well as the mathematical issues underlying the formulations of these models. The other type of model entails formulations based on the molecular mechanisms underlying the response. For example, in [19] Doi and Edwards developed a "reptation" model for concentrated solutions and polymer melts which is based on the assumption that an entangled polymer molecule, the chain,

slides (or reptates) through a "tube" whose contours are defined by the locus of entanglements with neighboring molecules. The polymer chain is free to diffuse along the tube axis but cannot move perpendicularly to the tube as other molecules restrict such movement. In [14] the polymer melt is modeled as a collection of interacting bead-rod chains. This model, referred to as the Curtiss-Bird model, is similar to the Doi-Edwards model, but it is based on a systematic kinetic development and does not use the phenomenological constraints of a chain in a tube. In addition, the comparison results of the Curtiss-Bird model and the Doi-Edwards model in [14] show that the the Curtiss-Bird model is more accurate than Doi-Edwards model in predicting the nonlinear behavior. A review of these molecular types of models as well as the relationship between the nonlinear viscoelasticity and molecular structure is given in [43].

In the following sections we restrict our discussions to those models that have been employed and developed by our group for understanding the dynamic response of the highly filled rubber and propagation of arterial stenosis induced shear waves in composite biotissue. The forms of these constitutive equations can be easily incorporated into the equation of motion so that we can numerically solve a partial differential equation with appropriate boundary and initial conditions to understand the dynamic behavior of materials.

Modified Boltzmann superposition model

The most direct formulation to treat nonlinear viscoelasticity is one based on generalizing the Boltzmann superposition model (3.19) to a corresponding nonlinear version. That is, one allows nonlinear instantaneous strain as well as nonlinear strain rate dependence. This "modified" superposition principle was first suggested in [34] where it was observed the creep behavior of fibres could be separated into time and stress-dependent parts, and then considered in [22] for a multiple-step test (in this regard see also the numerous contributions of Schapery as discussed in [51–53]). One form of this approach has been employed in some of our earlier efforts [9, 10] for modeling hysteretic damping in elastomers and is given by

$$\sigma(t) = g_e(\varepsilon(t)) + c_D\dot{\varepsilon}(t) + \int_0^t K(t-s)\frac{d}{ds}g_v\big(\varepsilon(s),\dot{\varepsilon}(s)\big)ds, \tag{3.27}$$

where ε is the infinitesimal strain, K is the convolution memory kernel, and g_e and g_v are nonlinear functions accounting for the elastic and viscoelastic responses of the materials, respectively. As explained in [9], our nonlinear materials undergoing large deformations required the use of finite (as opposed to infinitesimal) strain theories. However, since the nonlinearity between the stress and finite strain is an unknown and is to be estimated (using inverse problem algorithms) and since the finite strain can be expressed in terms of known nonlinearities as a function of the infinitesimal strain (at least in the problems of interest here), one can effectively formulate the problem as one of estimating the unknown nonlinearity between stress and infinitesimal strain. Thus one can develop nonlinear models for large deformation-related stress in terms of infinitesimal strain.

Again, this form of model (3.27), when incorporated into force balance laws (equation of motion), results in integro-partial differential equations which are computationally challenging both in simulation and control design. This motives us to employ the internal variable approach described below as an alternative for computation.

Fung's quasi-linear viscoelastic formulation

This formulation can be found in Fung [25] in the context of efforts to model soft tissue, which is often characterized by a constant hysteresis over a wider frequency range. In this formulation, a continuous spectrum over a finite range (τ_1, τ_2) is used to describe this phenomenon instead of using a finite spectrum $\{\tau_1, \tau_2, \cdots, \tau_n\}$ associated with relaxation kernels of the form given in (3.22). Fung's model is given by

$$\sigma(t) = \int_0^t K(t-\tau)\frac{d\sigma^e(\lambda(\tau))}{d\tau}d\tau. \tag{3.28}$$

Here the stress σ is the force in the deformed configuration divided by the cross-sectional area of the speciman at the zero stress state (i.e., the scalar version of the first Piola-Kirchhoff stress tensor), λ is the ratio of the length of the specimen stretched under the load divided by the initial length at the zero stress state, σ^e is the "elastic" response to this elongation, and $K(t)$ is the reduced relaxation function ("reduced" refers to that $K(t)$ is normalized such that $K(0) = 1$). Fung proposes a kernel of the form

$$K(t) = \frac{1 + c\int_{\tau_1}^{\tau_2}\frac{1}{\tau}\exp\left(\frac{-t}{\tau}\right)d\tau}{1 + c\ln(\tau_2/\tau_1)}, \tag{3.29}$$

where c represents the degree to which viscous effects are present, and τ_1 and τ_2 represent fast and slow viscous time phenomena.

Since its introduction, this quasi-linear viscoelastic (QLV) theory of Fung has been applied successfully in stress-strain experiments to several types of biological tissue. A benefit to using (3.28) as a constitutive equation is that, unlike simpler models for viscoelasticity, it allows for the consideration of a continuous spectrum (e.g., see the discussions in [25]) of relaxation times; this is also true of the probabilistic-based internal variable approach developed in [8] and described below. The need for a continuum of relaxation times in certain materials was observed many years ago (e.g., see [21, 29, 55]). While Fung's theory has been successfully employed for fitting hysteretic stress-strain curves, for control applications one is interested in using it in a full dynamical model. Unfortunately, the QLV theory, as presented by Fung, leads to exceedingly difficult computations within full dynamical partial differential equations, especially in estimation and control problems.

Internal variable approach

To overcome the computational challenges present in the modified Boltzmann superposition model and Fung's quasi-linear viscoelastic model, we turn to an internal variable approach in an alternative way to formulate the constitutive equation.

We observe that if the relaxation response kernel function K in model (3.27) is defined as in (3.22), then (3.27) can be written in terms of internal strains similar to (3.23) with (3.24):

$$\sigma(t) = g_e(\varepsilon(t)) + c_D\dot{\varepsilon}(t) + \sum_{j=1}^{n} \kappa_j \varepsilon_j(t), \tag{3.30}$$

where the internal strains ε_j satisfies

$$\frac{d\varepsilon_j(t)}{dt} + \frac{1}{\tau_j}\varepsilon_j(t) = g_v\big(\varepsilon(t), \dot{\varepsilon}(t)\big), \quad \varepsilon_j(0) = 0, \quad j = 1, 2, \cdots, n. \tag{3.31}$$

Through comparison with experimental data, in [10] it was discovered that the best fit to filled elastomer data occurs when g_e and g_v are cubic. Moreover, model (3.30) with (3.31) can be readily generalized to models with a continuum of relaxation times (see [12] and the references therein). These models have been useful in a wide range of viscoelastic materials. The corresponding stress-strain laws have the form

$$\sigma(t; \mathcal{P}) = g_e(\varepsilon(t)) + c_D\dot{\varepsilon}(t) + \gamma \int_{\mathcal{T}} \varepsilon_1(t; \tau) d\mathcal{P}(\tau), \tag{3.32}$$

where $\mathcal{P}$ is a probability distribution over the set $\mathcal{T}$ of possible relaxation parameters τ, and $\varepsilon_1(t; \tau)$ satisfies, for each $\tau \in \mathcal{T}$,

$$\frac{d\varepsilon_1(t; \tau)}{dt} + \frac{1}{\tau}\varepsilon_1(t; \tau) = g_v(\varepsilon(t), \dot{\varepsilon}(t)), \quad \varepsilon_1(0; \tau) = 0. \tag{3.33}$$

We also observe that if the reduced relaxation function $K(t)$ in Fung's QLV model (3.28) is defined as in (3.22) with

$$\sum_{k=1}^{n} \kappa_j = 1,$$

then model (3.28) is equivalent to the following internal strain variable formulation

$$\sigma(t) = \sum_{j=1}^{n} \kappa_j \varepsilon_j(t), \tag{3.34}$$

with the internal strains ε_j satisfying

$$\frac{d\varepsilon_j(t)}{dt} + \frac{1}{\tau_j}\varepsilon_j(t) = \frac{d\sigma^e(\lambda(t))}{dt}, \quad \varepsilon_j(0) = 0, \quad j = 1, 2, \cdots, n. \tag{3.35}$$

Various internal strain variable models are investigated in [1] and a good agreement is demonstrated between a two internal strain variable model (i.e., $n = 2$) and undamped simulated data based on the Fung kernel (3.29). The corresponding stress-strain laws for a generalization of these models to have a continuum of relaxation times have the form

$$\sigma(t; \mathcal{P}) = \int_{\mathcal{T}} \varepsilon_1(t; \tau) d\mathcal{P}(\tau), \tag{3.36}$$

where once again $\mathcal{P}$ is a probability distribution over the set $\mathcal{T}$ of possible relaxation parameters τ, and $\varepsilon_1(t;\tau)$ satisfies, for each $\tau \in \mathcal{T}$,

$$\frac{d\varepsilon_1(t;\tau)}{dt} + \frac{1}{\tau}\varepsilon_1(t;\tau) = \frac{d\sigma^e(\lambda(t))}{dt}, \qquad \varepsilon_1(0;\tau) = 0. \tag{3.37}$$

Molecular type of constitutive equations

Even though model (3.30) combined with (3.31) provides a reasonable fit to the experimental data, it does not provide insight into the underlying mechanisms for tensile and/or shear deformations in filled rubber. This is not unexpected since model (3.30)-(3.31) is based on pseudo-phenomenological formulations. Hence, a different approach based on molecular arguments was pursued in [4–6], where the ideas of these models are based on those of Johnson and Stacer in [32]. It turns out that this approach leads precisely to a class of models based on a Boltzmann formulation.

A polymer material undergoing directional deformation is modeled in [2] in which polymer chains are treated as Rouse type strings of beads interconnected by springs (see [49]) as depicted in the left plot of Fig. 19. The model permits the incorporation of many important physical parameters (such as temperature, segment bond length, internal friction, and segment density) in the overall hysteretic constitutive relationship. The model in [2] was based on the assumption that the materials were composed of two virtual compartments as depicted in the right plot of Fig. 19. One compartment consists of a constraining tube which is a macroscopic compartment containing both CC (chemically cross-linked) and PC (physically constrained) molecules. The other compartment is microscopic in nature and consist of those PC molecules aligned with the direction of the deformation. These molecules will at first "stick" to the constraining tube and be carried along with its motion, but will very quickly "slip" and begin to "relax" back to a configuration of lower strain energy. In the model derivation one computes the contributions of both "compartments" to the overall stress of this poly-

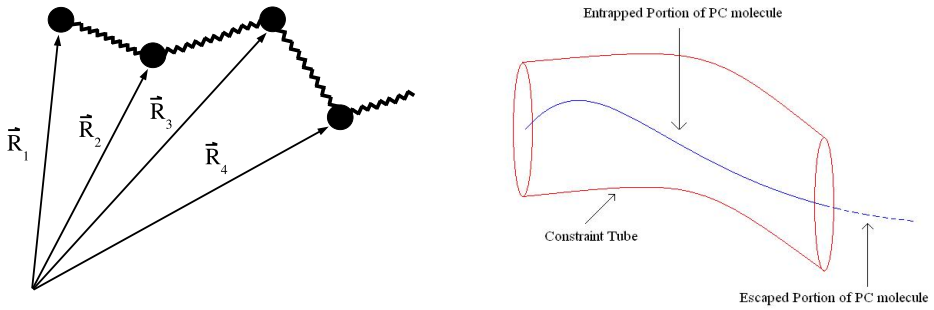

(a) (b)

Figure 19: (a): Representation of vectors for a bead-spring polymer molecule; (b): PC molecule entrapped by the surrounding constraining tube.

mer material undergoing deformations to obtain the constitutive law, which is similar to that developed in [4, 5] and has the general form of Boltzmann type model (3.27), even though the kernel is not of convolution type.

4 Examples

We have introduced and briefly discussed a number of possible constitutive relationships that represent a noncomprehensive review of an extensive body of research literature on elastic/viscoelastic materials. We conclude by presenting an example to illustrate how one might apply the equations of motion and a constitutive relationship to model a particular situation. In our computational example, we will examine the properties of a one dimensional column of dry soil and study the movement of the soil in response to a sinusoidal input at the surface. At first, we will record displacements in a wave moving past a stationary observation point in the soil column. We then add a rigid body to the column to demonstrate the changes in wave propagation one might expect if something is buried in the soil. We can change parameters, such as soil density, and understand the impact these changes have on the displacements at the observation point. In all cases, we focus on "seismic P waves" (longitudinal waves) propagating downward through the soil away from the source of the force (an impact) located at the ground surface.

4.1 Model description

The schematic for this problem is given on the left side of Fig. 20 where the wave observation point is at the location $z = z_{10}$ and the ground surface (as well as the source of the sinusoidal input force) is at $z = z_{p0}$. The right side of the figure represents the idealized (1-dimensional) mathematical soil column with input source and observation point marked in the figure. In the case where we have a rigid object in the soil, that object is placed at $z = z_{10}$ in the column instead of an observation point.

In this idealized configuration, we assume that both soil and target are uniform in x- and y-directions. Based on the discussion in Remark 3.4, we assume that soil

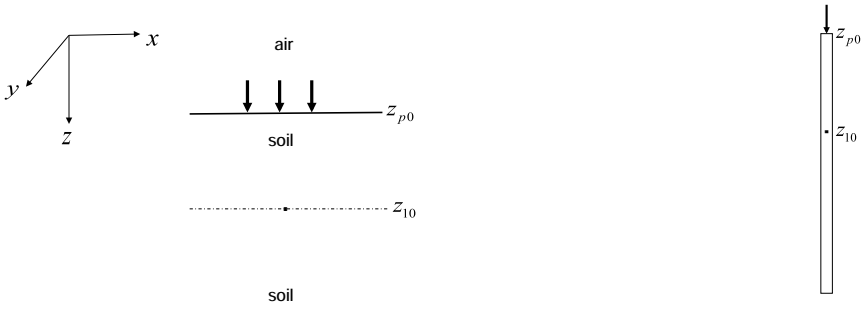

Figure 20: (left): Schematic of problem; (right): 1-dimensional representation.

behaves as a Kelvin-Voigt material for small vibrations. This means that stress components in soil can be expressed as sum of two terms, the first term being proportional to the strain (ε) and the second term being proportional to the rate of change ($\dot{\varepsilon}$) of strain.

Let $u(z,t)$ denote the displacement (in units m) in the z-direction at position z at time t. Then in the situation with no buried object, for $z \in (z_{p0}, \infty)$ we have

Case 1: Only soil present in the column

$$\rho(z)\frac{\partial^2 u(z,t)}{\partial t^2} = \frac{\partial}{\partial z}\Big(\kappa(z)\frac{\partial u(z,t)}{\partial z} + \eta(z)\frac{\partial^2 u(z,t)}{\partial t \partial z}\Big). \tag{4.1}$$

For a second case, we assume there is a buried rigid object with its center of mass located at $z = z_{10}$. We assume that the target is homogeneous in the z-direction, and the contacting surface area between the target and the soil under the target is the same as the one between the target and the soil above the target. Since the target is a rigid body, the displacement of upper side of the target is exactly the same as that of its lower side. Hence, in the 1-dimensional setting we can treat the target as a point mass. With the given assumptions on soil and target we can visualize the soil-target-soil as two thin rods connected by a point mass at $z = z_{10}$. The schematic of the problem is illustrated in the right plot of Fig. 20, where in this case there is a point mass at $z = z_{10}$. The resulting pair of equations are

Case 2: A rigid target present in the soil column

$$\rho(z)\frac{\partial^2 u(z,t)}{\partial t^2} = \frac{\partial}{\partial z}\Big(\kappa(z)\frac{\partial u(z,t)}{\partial z} + \eta(z)\frac{\partial^2 u(z,t)}{\partial t \partial z}\Big), \quad z \in (z_{p0}, z_{10}) \cup (z_{10}, \infty), \tag{4.2a}$$

$$\begin{aligned} M\frac{\partial^2 u(z_{10},t)}{\partial t^2} &= S\Big(\kappa(z_{10}^+)\frac{\partial u(z_{10}^+,t)}{\partial z} + \eta(z_{10}^+)\frac{\partial^2 u(z_{10}^+,t)}{\partial t \partial z}\Big) \\ &\quad - S\Big(\kappa(z_{10}^-)\frac{\partial u(z_{10}^-,t)}{\partial z} + \eta(z_{10}^-)\frac{\partial^2 u(z_{10}^-,t)}{\partial t \partial z}\Big). \end{aligned} \tag{4.2b}$$

In all cases ρ denotes the density (in units kg/m^3) of soil, κ is the elastic modulus (in units kg/m$\cdot$ s ^{2} = Pa) of soil , and η represents the damping coefficient (in units kg/m $\cdot$ s) of soil. For the second equation in (4.2), M is used to denote the mass (in units kg) of the target and S represents the surface area (in units m^2) of contact between the target and the soil under (or above) the target. Though the model will treat non-constant and piecewise-defined coefficients, for our example we will take the simple case where the parameters are constant values in the soil column. In general, non-constant and piecewise-defined coefficients would allow one to account for varying physical situations, such as having a lower density above a buried object than below the buried object. For initial conditions we will assume zero displacement and zero velocity since the system is at rest initially. These conditions are then given by

$$u(z,0) = 0, \qquad \frac{\partial u}{\partial t}(z,0) = 0. \tag{4.3}$$

The boundary condition at $z = z_{p0}$ is given by

$$\left(\kappa(z)\frac{\partial u(z,t)}{\partial z} + \eta(z)\frac{\partial^2 u(z,t)}{\partial t \partial z}\right)\Big|_{z=z_{p0}} = -f(t), \tag{4.4}$$

where f is the applied external force in units $\mathrm{N/m^2}$. On the surface, the normal internal stress is balanced with the input force, resulting in (4.4).

In order to numerically solve our model (4.1) with (4.3) and (4.4) or model (4.2) with (4.3) and (4.4), it is convenient to have a finite spatial domain. Since we only care about the displacements near the surface (and near the buried object in the second case), we will choose the right (lower) boundary z_{00} to be sufficiently far away from the target so that no energy will reach the boundary z_{00} during the time frame within which we run the simulations. This assumption implies that we can set up any type of boundary condition at z_{00}. For simplicity, we assume that

$$u(z_{00}, t) = 0. \tag{4.5}$$

Hence, our problem (4.1) with (4.3) and (4.4), and problem (4.2)-(4.4) is thus defined on the finite space domain $[z_{p0}, z_{00}]$. We report on computations for the model using a standard finite element method.

4.2 Simulation results

We report the results of some of our simulations with the equations governing this one layer problem, observing the wave form through time at location $z_{10} = 0.3048\mathrm{m}$, which is approximately one foot beneath the ground surface at $z_{p0} = 0$. The value for the far boundary was set at 50m, and no reflections from the far boundary were observed in the calculations. The baseline numerical values for soil density and elastic modulus are

$$\rho = 1800\mathrm{kg/m^3}, \qquad \kappa = 2.04 \times 10^8\ \mathrm{Pa}, \tag{4.6}$$

where the values were estimated from [17]. For the value of damping coefficient of soil η, we will assume that damping is frequency- and elastic modulus-dependant, via the formula

$$\eta = \frac{2\beta\kappa}{\omega\sqrt{1-\beta^2}}. \tag{4.7}$$

The parameter β is called the damping ratio, which is related to the energy lost between wave peaks. The baseline value for the damping ratio was set at $\beta = 0.05$, which again was derived using results from [17]. For the carrier frequency in our simulations, we apply the sinusoidal input function at a frequency of $\omega = 400\pi$.

We depict a plot of a sinusoidal input function in Fig. 21. Recall that, given our coordinate system, positive force values represent downward force and negative force values represent upward force. Thus, this input represents impacting the ground in a downward motion and then the ground rebounding with equal force. We can thus see

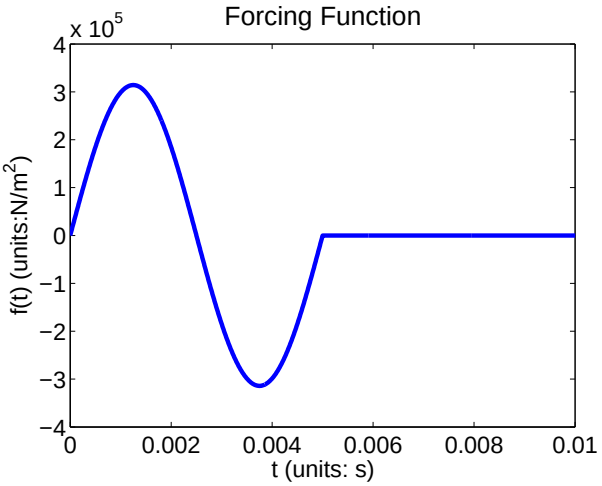

Figure 21: Sinusoidal input function.

displacement return to the baseline in all of the following figures due to the restoring force present in the input. Since the displacement returns to the baseline, we can also infer that our model is linearly dependent on the input.

We remark that the input term and the equations we use for demonstration purposes are only a convenient approximation to physical reality in a small displacements case. One could implement the actual physical situation by allowing for a *moving upper boundary* at z_{p0}. In this case, the input would only be the first, positive part of the sine wave, as the differential equation dynamics coupled with the moving boundary would return the soil to near its original position. Since a moving boundary is more difficult to implement computationally, for this demonstration we chose to implement the simpler stationary boundary at the impact site z_{p0}. In reality, the ground boundary will not remain stationary under impact, but it will instead move first in the positive (downward) direction and then rebound in the negative (upward) direction. The rebound is due in part to the viscoelastic properties of the soil column and also to the physical soil column interacting with the surrounding soil (e.g., shear which is not represented explicitly in the one dimensional dynamics). We model this restoring motion as the second half of the input signal as depicted in Fig. 21. That is, the positive first half of the sinusoid represents the force imparted by the thumper and the negative latter half is modeling the rebounding of the soil boundary that one would (and we did in field experiments) see in reality. This permits use of the stationary boundary at z_{p0} while still approximating (with reasonable accuracy) the true dynamics at the surface.

4.2.1 Results for Case 1: only soil present in the column

The first situations we examine are when holding one parameter (of (κ, ρ)) constant and increase the other parameter. The results are depicted in the panels of Fig. 22. In the left panel, we hold density ρ constant and change the elastic modulus κ. As

the modulus increases, we see that the wave begins its upward slope sooner, meaning the wave has arrived at the observation point sooner so wave speed has increased. Also, as the modulus increases, we see less displacement overall. In the case where density increases, we see that we also get less displacement overall, but the wave speed decreases. We clearly see the model demonstrates that soil parameters have multiple realistic effects on overall displacement and wave speed.

In Fig. 23, we examine the situation where we increase both soil parameters. As expected, the effects of the parameter increases combine to reduce overall displacement. In the left pane of the figure, we see that the elastic modulus increases more rapidly than the density and the wave reaches the observation point sooner. In the right pane, we applied the same percentage increases to the parameters and so the wave reaches the observation point at the same time for all the parameter combinations. Thus, our model is able to demonstrate the effects of more complex parameter changes that one might see in applications. For example one might input multiple impacts at the same site, which would increase both soil density and stiffness from one impact to the next. (This in fact was realized in field experiments by scientific colleagues when testing for repeatability of responses to interrogation impacts.)

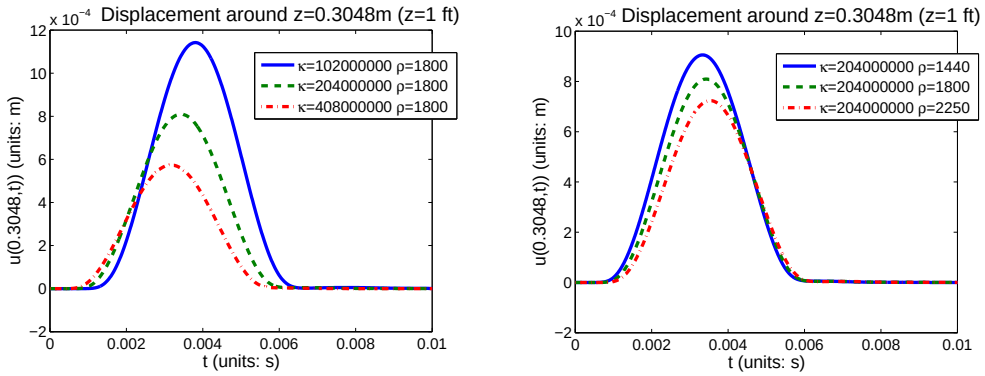

Figure 22: Wave form at z_{10} with varying soil parameters individually (left: variable κ, constant ρ; right: constant κ, variable ρ).

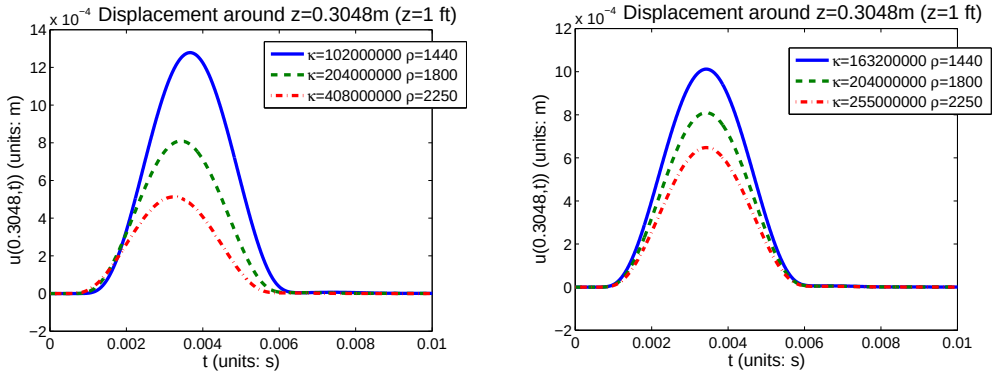

Figure 23: Wave form at z_{10} with both soil parameters κ and ρ varying.

4.2.2 Results for Case 2: rigid body present in the soil column

In this section we examine the case where we have included a rigid body located at z_{10}, modeled as a point mass at the same point as our previous observation point. In the figures, this location is represented by a vertical dashed line. For all the simulation results presented in this section, the values for the soil density, elastic modulus and damping ratio are chosen to be the baseline values specified earlier, with the value for the mass of the target given by $M = 34.2671$kg, and the contacting surface area taken as $S = 0.1580\text{m}^2$.

In the upper left pane of Fig. 24, we can see that the sinusoidal force has begun imparting displacement in the soil but this displacement has not yet reached the target. In the upper right pane, the displacement has impacted the target. In this simulation, the target imparts much of the energy to the soil below it. In the lower left pane of Fig. 24, we see that most of the energy has passed through the target and is deeper into the soil. However, looking at the domain between $z = 0$ and the dashed target line, we see the remnant energy that was reflected by the target back toward the surface. In the lower right pane in the figure, we see that this energy has bounced off the soil and impacted the target again, once more passing some energy through the target (as seen

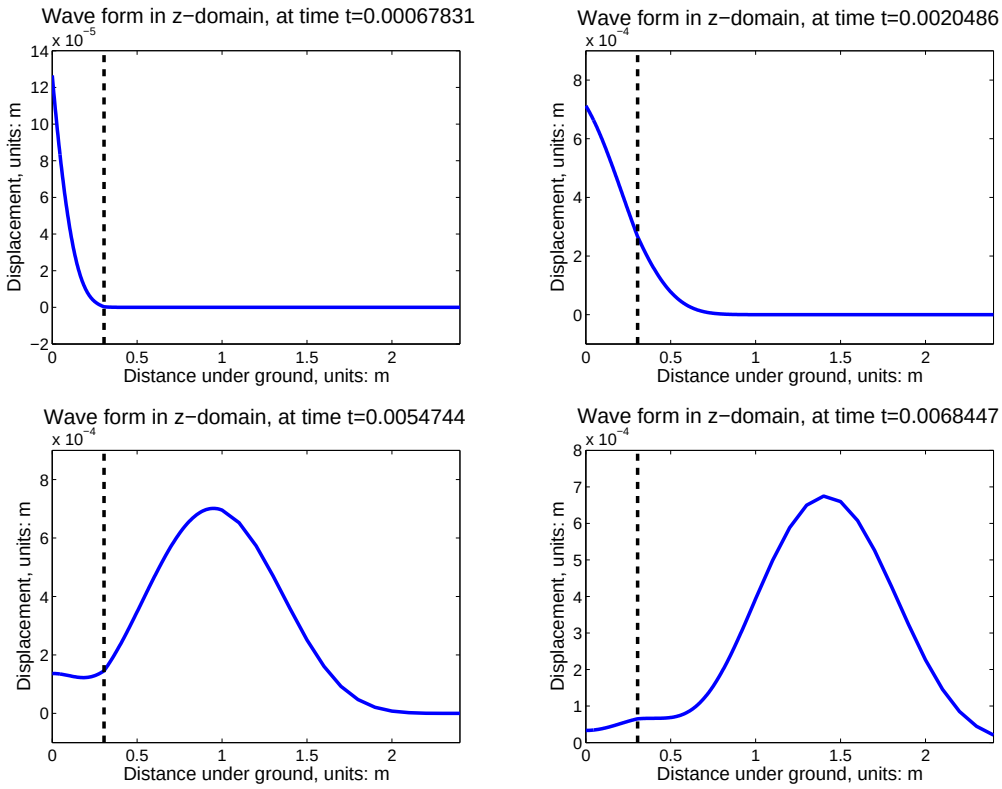

Figure 24: Wave form in the soil column at various times (the buried object location is represented by vertical dashed line).

in the small amount of extra displacement to the right of the dashed line) and having some energy reflected. The basic one dimensional model we have used can effectively model the presence of a rigid body in a column of soil, in particular the behavior of partial reflecting and transmitting of energy when the object is impacted.

This numerical example has demonstrated the ability of a one dimensional model to capture some of the salient features of wave propagation in the soil medium, including sensitivity to soil structure and to the presence of rigid objects in the soil. Additional features that would require a two or three dimensional model might be modeling the presence of more than one type of body wave (e.g., shear and compressional) as well as modeling surface waves. In such a higher dimensional setting we could also take into account more complicated buried object geometries. Ultimately, the one dimensional model still captures much of the basic dynamics of elasticity in soil and is therefore useful in predicting outcomes to physical experiments with some degree of fidelity.

Acknowledgments

This research was supported in part by the Air Force Office of Scientific Research under grant number FA9550-09-1-0226. The efforts of ZRK were supported in part by the Department of Education with a GAANN Fellowship under grant number P200A070386. The authors are grateful to Dr. Richard Albanese for encouragement, suggestions and constructive comments during the course of preparation of the material in this manuscript.

References

[1] H. T. Banks, J. H. Barnes, A. Eberhardt, H. Tran and S. Wynne, *Modeling and computation of propagating waves from coronary stenoses*, Comput. Appl. Math., 21 (2002), pp. 767–788.

[2] H. T. Banks, J. B. Hood, N. G. Medhin and J. R. Samuels, *A stick-slip/Rouse hybrid model for viscoelasticity in polymers*, Technical Report CRSC-TR06-26, NCSU, November, 2006, Nonlinear. Anal. Real., 9 (2008), pp. 2128–2149.

[3] H. T. Banks and N. Luke, *Modelling of propagating shear waves in biotissue employing an internal variable approach to dissipation*, Commun. Comput. Phys., 3 (2008), pp. 603–640.

[4] H. T. Banks, N. G. Medhin and G. A. Pinter, *Nonlinear reptation in molecular based hysteresis models for polymers*, Quart. Appl. Math., 62 (2004), pp. 767–779.

[5] H. T. Banks, N. G. Medhin and G. A. Pinter, *Multiscale considerations in modeling of nonlinear elastomers*, Technical Report CRSC-TR03-42, NCSU, October, 2003, J. Comp. Meth. Engr. Sci. Mech., 8 (2007), pp. 53–62.

[6] H. T. Banks, N. G. Medhin and G. A. Pinter, *Modeling of viscoelastic shear: a nonlinear stick-slip formulation*, CRSC-TR06-07, February, 2006, Dyn. Sys. Appl., 17 (2008), pp. 383–406.

[7] H. T. BANKS AND G. A. PINTER, *Damping: hysteretic damping and models*, CRSC-TR99-36, NCSU, December, 1999; Encyclopedia of Vibration (S. G. Braun, D. Ewins and S. Rao, eds.), Academic Press, London, 2001, pp. 658–664.
[8] H. T. BANKS AND G. A. PINTER, *A probabilistic multiscale approach to hysteresis in shear wave propagation in biotissue*, Mult. Model. Sim., 3 (2005), pp. 395–412.
[9] H. T. BANKS, G. A. PINTER, L. K. POTTER, M. J. GAITENS AND L. C. YANYO, *Modeling of quasistatic and dynamic load responses of filled viscoelastic materials*, CRSC-TR98-48, NCSU, December, 1998; Chapter 11 in Mathematical Modeling: Case Studies from Industry (E. Cumberbatch and A. Fitt, eds.), Cambridge University Press, 2001, pp. 229–252.
[10] H. T. BANKS, G. A. PINTER, L. K. POTTER, B. C. MUNOZ AND L. C. YANYO, *Estimation and control related issues in smart material structures and fluids*, CRSC-TR98-02, NCSU, January, 1998, Optimization Techniques and Applications (L. Caccetta, et al., eds.), Curtain Univ. Press, July, 1998, pp. 19–34.
[11] H. T. BANKS AND J. R. SAMUELS, JR., *Detection of cardiac occlusions using viscoelastic wave propagation*, CRSC-TR08-23, North Carolina State University, 2008; AAMM., 1 (2009), pp. 1–28.
[12] H. T. BANKS, *A brief review of some approaches to hysteresis in viscoelastic polymers*, CRSC-TR08-02, January, 2008; Nonlinear. Anal. Theor., 69 (2008), pp. 807–815.
[13] J. P. BARDET, *A viscoelastic model for the dynamic behavior of saturated poroelastic soils*, J. Appl. Mech. ASME., 59 (1992), pp. 128–135.
[14] R. B. BIRD, C. F. CURTISS, R. C. ARMSTRONG AND O. HASSAGER, Dynamics of Polymeric Liquids, Vol. 2, Kinetic Theory, Wiley, New York, 1987.
[15] M. A. BIOT, *Theory of propagation of elastic waves in a fluid saturated porous solid*, J. Acust. Soc. Am., 28 (1956), pp. 168–191.
[16] R. M. CHRISTENSEN, Theory of Viscoelasticity, 2nd ed., Academic Proess, New York, 1982.
[17] N. CHOUW AND G. SCHMID, Wave Propagation, Moving Load, Vibration Reduction: Proceedings of the International Workshop WAVE 2002, Okayama, Japan, 18-20 September 2002, Taylor & Francis, 2003.
[18] M. A. DEL NOBILE, S. CHILLO, A. MENTANA AND A. BAIANO, *Use of the generalized Maxwell model for describing the stress relaxation behavior of solid-like foods*, J. Food. Eng., 78 (2007), pp. 978–983.
[19] M. DOI AND M. EDWARDS, The Theory of Polymer Dynamics, Oxford, New York, 1986.
[20] C. S. DRAPACA, S. SIVALOGANATHAN AND G. TENTI, *Nonlinear constitutive laws in viscoelasticity*, Math. Mech. Solids., 12 (2007), pp. 475–501.
[21] J. D. FERRY, E. R. FITZGERALD, L. D. GRANDINE AND M. L. WILLIAMS, *Temperature dependence of dynamic properties of elastomers: relaxation distributions*, Ind. Engr. Chem., 44 (1952), pp. 703–706.
[22] W. N. FINDLEY AND J. S. Y. LAI, *A modified superposition principle applied to creep of nonlinear viscoelastic materials under abrupt changes in state of combined stress*, Trans. Soc. Rheol., 11 (1967), pp. 361–380.
[23] W. N. FINDLEY, J. S. LAI AND K. ONARAN, Creep and Relaxation of Nonlinear Viscoelastic Materials, Dover Publications, New York, 1989.
[24] Y. C. FUNG, Foundations of Solid Mechanics, Prentice-Hall, Englewood Cliffs, NJ, 1965.
[25] Y. C. FUNG, Biomechanics: Mechanical Properties of Living Tissue, Springer-Verlag, Berlin, 1993.
[26] Y. C. FUNG, A First Course in Continuum Mechanics, Prentice Hall, New Jersey, 1994.
[27] A. E. GREEN AND R. S. RIVLIN, *The mechanics of non-linear materials with memory*, Arch.

Ration. Mech. An., 1 (1957), pp. 1–21.
[28] M. GURTIN AND E. STERNBERG, *On the linear theory of viscoelasticity*, Arch. Ration. Mech. An., 11 (1965), pp. 291–365.
[29] D. TER HAAR, *A phenomenological theory of viscoelastic behavior*, Phys., 16 (1950), pp. 839–850.
[30] Y. M. HADDAD, Viscoelasticity of Engineering Materials, Chapman & Hall, Dordrecht, Netherlands, 1995.
[31] B. O. HARDIN, *The nature of damping in sands*, J. Soil Mech. Found. Div., 91 (1965), pp. 63–97.
[32] A. R. JOHNSON AND R. G. STACER, *Rubber viscoelasticity using the physically constrained systems stretches as internal variables*, Rubber. Chem. Technol., 66 (1993), pp. 567–577.
[33] R. S. LAKES, Viscoelastic Solids, CRC Press, Boca Raton, FL, 1998.
[34] H. LEADERMAN, Elastic and Creep Properties of Filamentous Materials, Textile Foundation, Washington, D.C., 1943.
[35] P. LE TALLEC, Numerical Analysis of Viscoelastic Problems, Masson/Springer-Verlag, Paris/Berlin, 1990.
[36] P. LE TALLEC, C. RAHIER AND A. KAISS, *Three-dimensional incompressible viscoelasticity in large strains: formulation and numerical approximation*, Comput. Meth. Appl. Mech. Eng., 109 (1993), pp. 233–258.
[37] F. J. LOCKETT, Nonlinear Viscoelastic Solids, Academic, New York, 1972.
[38] N. LUKE, Modeling Shear Wave Propagation in Biotissue: An Internal Variable Approach to Dissipation, Ph.D. thesis, North Carolina State University, Raleigh, NC, `http://www.ncsu.edu/grad/etd/online.html`, 2006.
[39] J. E. MARSDEN AND T. J. R. HUGHES, Mathematical Foundations of Elasticity, Prentice-Hall, Englewood Cliffs, NJ, 1983.
[40] P. MICHAELS, *Relating damping to soil permeability*, Int. J. Geomech., 6 (2006), pp. 158–165.
[41] P. MICHAELS, *Water, inertial damping, and complex shear modulus*, Geotech. SP., 2008.
[42] K. N. MORMAN. JR., *Rubber viscoelasticity-a review of current understanding*, Proceedings of the Second Symposium on Analysis and Design of Rubber Parts, Jan. 14–15, 1985.
[43] J. G. OAKLEY, A. J. GIACOMIN AND J. A. YOSICK, *Molecular origins of nonlinear viscoelasticity: fundamental review*, Mikrochimica. Acta., 130 (1998), pp. 1–28.
[44] R. W. OGDEN, Non-Linear Elastic Deformations, Dover Publications, 1984.
[45] A. P. PENNERU, K. JAYARAMAN AND D. BHATTACHARYYA, *Viscoelastic behaviour of solid wood under compressive loading*, Holzforschung., 60 (2006), pp. 294–298.
[46] A. C., PIPKIN AND T. G. ROGERS, *A non-linear integral representation for viscoelastic behaviour*, J. Mech. Phys. Solids., 16 (1968), pp. 59–72.
[47] F. E. RICHART AND J. R. WOODS, Vibrations of Soils and Foundations, Prentice Hall, NJ, 1970.
[48] R. S. RIVLIN, *Large elastic deformations of isotropic materials, I, II, III*, Phil. Trans. Roy. Soc. A., 240 (1948), pp. 459–525.
[49] P. E. ROUSE. JR., *A theory of the linear viscoelastic properties of dilute solutions of coiling polymers*, J. Chem. Phys., 21 (1953), pp. 1272–1280.
[50] J. R. SAMUELS, Inverse Problems and Post Analysis Techniques for a Stenosis-Driven Acoustic Wave Propagation Model, Ph.D. thesis, North Carolina State University, Raleigh, NC, `http://www.ncsu.edu/grad/etd/online.html`, 2008.
[51] R. A. SCHAPERY, *On the characterization of nonlinear viscoelastic solids*, Polymer. Eng. Sci., 9 (1969), pp. 295–310.
[52] R. A. SCHAPERY, *Nonlinear viscoelastic and viscoplastic constitutive equations based on ther-*

modynamics, Mech. Time-Depend. Mat., 1 (1997), pp. 209–240.
[53] R. A. SCHAPERY, *Nonlinear viscoelastic solids*, Int. J. Solids. Struct., 37 (2000), pp. 359–366.
[54] C. T. SCHRODER, W. R. SCOTT, JR., AND G. D. LARSON, *Elastic waves interacting with buried land mines: a study using the FDTD method*, IEEE Trans. Geosci. Remote. Sens., 40 (2002), pp. 1405–1415.
[55] F. SCHWARZL AND A. J. STAVERMAN, *Higher approximation methods for the relaxation spectrum from static and dynamic measurements of viscoelastic materials*, Appl. Sci. Res., A4 (1953), pp. 127–141.
[56] W. R. SCOTT, G. D. LARSON AND J. S. MARTIN, *Simultaneous use of elastic and electromagnetic waves for the detection of buried land mines*, Proc. SPIE., 4038 (2000), pp. 1–12.
[57] T. H. SHELLHAMMER, T. R. RUMSEY AND J. M. KROCHTA, *Viscoelastic properties of edible lipids*, J. Food. Eng., 33 (1997), pp. 305–320.
[58] J. SMART AND J. G. WILLIAMS, *A comparison of single integral non-linear viscoelasticity theories*, J. Mech. Phys. Solids., 20 (1972), pp. 313–324.
[59] L. R. G. TRELOAR, The Physics of Rubber Elasticity, 3rd edition, Oxford University Press, 1975.
[60] C. TRUESDELL, Rational Thermodynamics, Springer, Berlin, 1984.
[61] A. WINEMAN, *Nonlinear viscoelastic solids-a review*, Math. Mech. Solids., 14 (2009), pp. 300–366.